A Molecular Theory for Fast Flows of Entangled Polymers

D. W. Mead*,‡ and R. G. Larson†

Departments of Chemical and Mechanical Engineering, University of Michigan, Ann Arbor, Michigan 48109-2136

M. Doi

Department of Applied Physics, Nagoya University, Nagoya, 464 Japan

Received January 29, 1998; Revised Manuscript Received August 21, 1998

ABSTRACT: The Doi−Edwards (DE) theory for the rheological properties of entangled polymer melts and solutions successfully predicts the response to large step-shear strains but fails to predict other nonlinear shear properties, such as the steady-state viscosity or the relaxation of stress after cessation of steady shearing. Many of these failures remain even in the extension of the theory by Marrucci and Grizzuti (*Gazz. Chim. Ital.* **1988**, *118*, 179)[1] to allow deformation-induced "tube stretch". Here, we find that a much more successful theory can be obtained by also accounting for "convective constraint release", i.e., the loss of entanglement constraints caused by the retraction of surrounding chains in their tubes. (Marrucci, G. *J. Non-Newtonian Fluid Mech.* **1996**, *62*, 279 and Ianniruberto, G.; Marrucci, G. *J. Non-Newtonian Fluid Mech.* **1996**, *65*, 241).[2,3] In the molecular model developed here, convective constraint release can both shorten the reptation tube and allow reorientation of interior tube segments. The revised model predicts many of the features of steady and transient shearing flows. These include a region of nearly constant steady-state shear stress at shear rates between the inverse zero-shear reptation time and the inverse Rouse time, similar to that seen in the experiments of Bercea et al. (*Macromolecules* **1993**, *26*, 7095)[4] and also predicted by Marrucci and Ianniruberto (*Macromol. Symp.* **1997**, *117*, 233).[5] The predictions of transient stresses after startup and cessation of shear are also in good agreement with experiments, as are predictions of nonmonotonicity in the extinction angle after stepup or stepdown in shear rate.

I. Introduction

The tube model and variations of it have proved highly successful in describing the linear viscoelastic properties of monodisperse and polydisperse entangled linear and star-branched polymers. The major mechanisms of relaxation included in these theories are (1) *reptation* of a linear polymer chain within the mesh of constraints created by the surrounding chains, (2) *fluctuation* of the length of the chain's "primitive path", or average contour, within the mesh of constraints, and (3) *release of the constraints* by motion of the surrounding chains.

For highly entangled, monodisperse, linear chains, reptation is the dominant mechanism for slow flows, and it gives a reasonably accurate prediction of the linear properties, especially if one also includes relaxation of chain ends due to fluctuations.[6] For polydisperse melts of linear chains, constraint release is important, since fast motions of short chains remove topological barriers and thus allow partial relaxation of long chains sooner than would otherwise occur.[7] Accurate, yet simple, predictions for melts of arbitrary polydispersity can be obtained using a simplified constraint-release description called "double reptation".[8−14]

For star polymers, reptation is suppressed, and relaxation occurs by a combination of fluctuations plus constraint release. Ball and McLeish[15] accounted for these mechanisms by developing the concept of "dynamic dilution", in which the gradual disappearance of constraints leads to a progressive widening of the tube. They thereby obtained predictions of the storage and loss moduli in excellent agreement with those of nearly monodisperse polyisoprene star melts over 4 decades of frequency. Presumably, a combination of fluctuations and constraint release could also describe the linear-relaxation properties of polydisperse star melts, and of mixtures of linear and star polymers, if reptation of the linear chains is accounted for. Thus, theories of the *linear* viscoelastic properties of entangled polymer melts are rather well developed.

Theories for *nonlinear* properties are much less advanced, however, even for the simplest case of monodisperse linear chains. The Doi−Edwards (DE) theory accounts for nonlinear viscoelastic properties of such chains by combining reptation with instantaneous and complete *chain retraction* within a mesh of constraints affinely deformed by the flow.[16−18] "Complete" chain retraction in the DE theory means that the length of the tube occupied by the chain remains constant in any flow. The predictions of the DE model for nonlinear *step-shear strains* are in excellent agreement with data for monodisperse, linear, entangled melts. However, in other deformation histories, including steady-state shear, the predictions do not agree even qualitatively with experiments (see below).

A refinement of the DE theory by Marrucci and Grizzuti, referred to as the DEMG theory,[1,19,20] allows chain retraction to be gradual and incomplete, so that the tube can be "stretched" by the flow. By "tube stretch", we mean that the length of tube occupied by the chain is increased above its equilibrium value. Locally, the flow always deforms the tube affinely, but at low strain rates the molecule retracts fast enough that the length of occupied tube does not change. The inclusion of tube stretch leads to improved predictions

† Department of Chemical Engineering.
‡ Department of Mechanical Engineering.

10.1021/ma980127x CCC: $15.00
Published on Web 10/16/1998

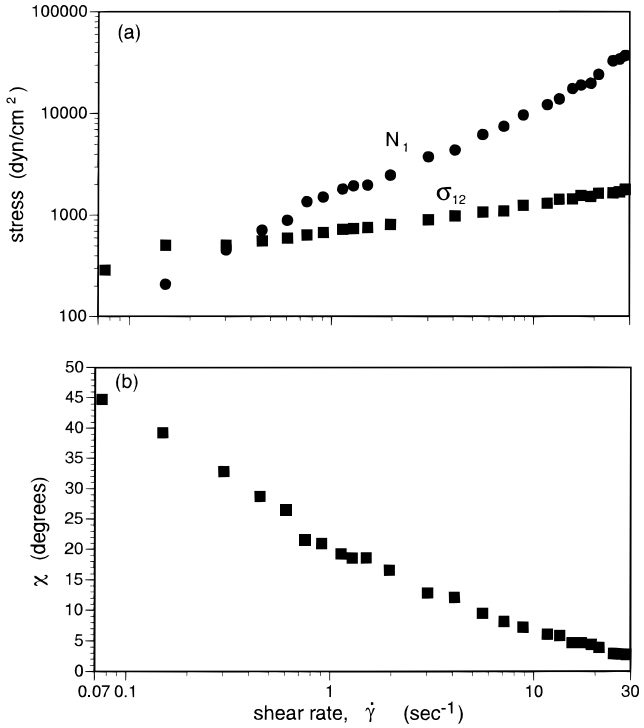

Figure 1. (a) Shear stress σ_{12} and first normal stress difference N_1 as functions of shear rate for a 3 wt % solution of 8.4×10^6 molecular-weight polystyrene in tricresyl phosphate at room temperature, obtained from optical measurements of birefringence and extinction (or orientation) angle in a circular Couette device described by Mead and Larson.[54] (b) Extinction ratio as a function of shear rate from the same measurements. The number of entanglements per molecule can be estimated from the formula $N = \phi M/M_e$, where ϕ is the polymer volume fraction, M its molecular weight, and M_e the entanglement spacing in the melt, given by $M_e \approx 13\,300$ for polystyrene according to Fetters et al.[53] This gives $N \approx 20$. From linear viscoelastic measurements, we find the Rouse time, τ_s, to be around 0.3 s; from the crossover of σ_{12} and N_1, we estimate the longest relaxation time τ_1 to be 2 s.

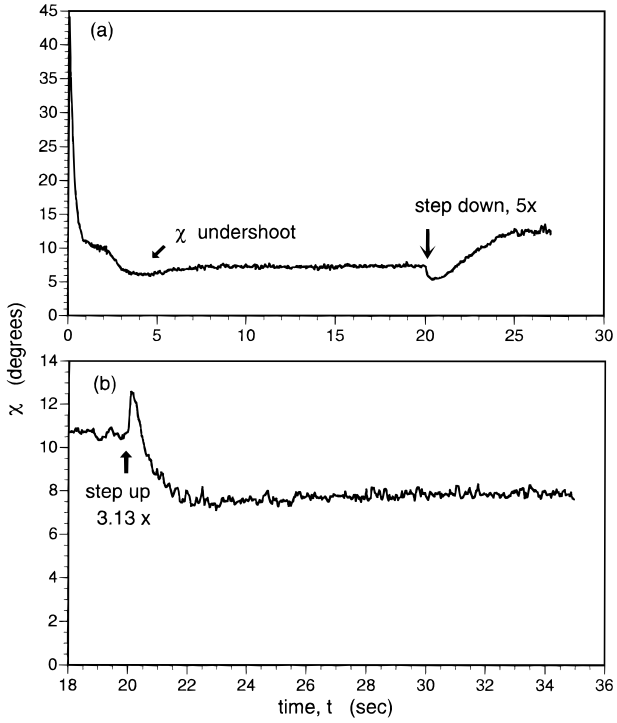

Figure 2. Transients in the extinction angle χ with time after startup of steady shearing and subsequent attainment of steady state, followed at 20 s by (a) a stepdown in shear rate by a factor of 5 from 9.44 s^{-1} ($\dot{\gamma}\tau_s \approx 3$) to 1.89 s^{-1} ($\dot{\gamma}\tau_s \approx 0.6$) and by (b) a stepup of shear rate from 3.02 s^{-1} ($\dot{\gamma}\tau_s \approx 1$) to 9.44 s^{-1} ($\dot{\gamma}\tau_s \approx 3$). In part a, the "shoulder" at around 2 s is an experimental artifact produced by the birefringence signal passing over an order of retardance (from Mead[29]).

of overshoots in the first normal stress difference N_1 and in the shear stress σ_{12}, and the correct dependences of the strains at maximum overshoot on shear rate[19] (assuming one of the parameters of the theory, the "Rouse" relaxation time, is adjusted arbitrarily by a factor of 4). However, the DEMG version does *not* remove the other failings of the DE theory.[21]

Important features of the nonlinear rheological behavior of linear polymers that the DE and DEMG theories fail to describe are as follows:

(1) Over a wide range of shear rates $\dot{\gamma}$ above the inverse reptation time $1/\tau_d$, the shear stress σ_{12} is nearly constant for very highly entangled melts or solutions[4] or increases slowly with shear rate for less highly entangled ones; see Figure 1a. The first normal stress difference N_1 increases more rapidly with shear rate than does the shear stress over the same range of shear rate; again see Figure 1a. The slope of N_1 versus $\dot{\gamma}$ also increases as the molecular weight decreases. The DE and DEMG theories, on the other hand, predict a maximum in σ_{12} followed by a region in which σ_{12} decreases with shear rate asymptotically as $\dot{\gamma}^{-0.5}$. $N_1(\dot{\gamma})$ is predicted by these theories to approach a constant at high $\dot{\gamma}$.

(2) Curves of shear viscosity versus shear rate for different molecular weights merge in the high-shear-rate, shear-thinning, regime nearly into a single curve; that is, there is only a very weak dependence of viscosity on molecular weight at high shear rate.[22−25] The DE and DEMG theories predict that at high shear rate in the shear-thinning region the melt viscosity actually *decreases* with increasing molecular weight.

(3) The steady-state value of the extinction angle χ, measured in birefringence or mechanically—see Figure 1b—falls more gradually than predicted by the DE theory. The extinction angle is the orientation angle that the dominant principal axis of the birefringence tensor makes with the flow direction. The extinction angle χ is given by (1/2) $\tan^{-1}[2n_{12}/(n_{11} - n_{22})]$ where n_{ij} are the components of the birefringence tensor **n**, with 1 and 2 representing the flow and flow-gradient directions, respectively. For melts and concentrated solutions of flexible polymers, these components are related to the shear stress σ_{12} and first normal stress difference N_1 via the stress-optical rule,[26] such that $\chi = (1/2)\tan^{-1}(2\sigma_{12}/N_1)$.

(4) In the nonlinear regime, the rate of relaxation of shear stress after cessation of steady-state shearing at a rate $\dot{\gamma}_0$ increases with the prior shear rate[27,28] $\dot{\gamma}_0$. The DE and DEMG theories predict that the relaxation rate is insensitive to $\dot{\gamma}_0$.

(5) After startup of fast steady shearing, the extinction angle undershoots before reaching steady state; see the first portion of the curve in Figure 2a. If, after a steady state has been reached, the shear rate is suddenly decreased, the extinction angle decreases before reaching a higher steady-state value (Figure 2a; second portion of curve). The reverse happens if the shear rate is suddenly increased (Figure 2b).[29] Such over- and undershoots are not predicted by the DE and DEMG theories.

These failures are no doubt related to each other; in particular, the failure described in point 2 can be shown to be a consequence of the excessive shear thinning described in point 1. Indeed, most of the failings occur because in fast shearing flow the theory predicts that the tube segments become highly oriented in the flow direction and hence present a very slim profile to the flow. As a result, the flow "loses its grip" on the molecules, leading to anomalously low friction and hence low viscosity. These failings are not relieved by inclusion of tube stretch via the DEMG theory. Indeed, although the DEMG theory predicts that in fast shearing the tube and the chain in it are (temporarily) highly stretched and therefore contribute to a high viscosity, the tube inevitably rotates to a small angle with respect to the flow direction, and then the drag on the chain collapses, leading to loss of tube stretch and a reduced viscosity. Thus, the failures of even the rather sophisticated DEMG version of the theory make clear how deep the problems with the DE theory truly are, especially in simple shearing flows.

Recently, Marrucci[2] has pinpointed what we believe is the key to the problem in the DE theory. He recognized that while *constraint release* may be a slow, and perhaps not so important, process when a monodisperse melt is at rest or undergoing slow flow, when there is a flow that is fast compared to the inverse of the reptation time, constraints surrounding a given chain are rapidly swept away, leaving the chain much more free to relax than is possible in pure reptation. Ianniruberto and Marrucci[3] refer to this mechanism as "convective constraint release", or CCR.

Despite this conceptual breakthrough, it has proven difficult to develop a complete theory, one capable of resolving all discrepancies described in points 1−5 while simultaneously retaining the satisfactory features of the existing theory, namely, the realistic behavior in step shear and in stress overshoots in startup of shear. Of course, one would also like, if possible, to avoid the use of ad hoc assumptions or adjustable parameters in order to retain the simplicity and universality of the original DE and DEMG theories, which have only the plateau modulus, reptation time, and Rouse retraction times as independent constants (and these are fixed by molecular characteristics and so cannot really be considered adjustable). Because of the theoretical difficulties achieving a complete theory, Marrucci and co-workers have developed models that incorporate plausible physical ideas, but in simplified form. An important simplification in such models is the neglect of the dependence of orientation and stretch on the tube coordinate of chain; i.e., it is assumed that all parts of the molecule share the same orientation and degree of stretch. While this approximation may seem severe, studies of such models will hopefully eventually lead to the discovery of a suitable complete theory.

In section II.A, we develop a new simplified model which we believe is an appropriate formulation of the CCR mechanism. We show in section II.B that this model retains the successful features of the DE theory and, in addition, captures the phenomena described in points 1−4. While the simplified model fails to capture the transients in χ described in point 5, we show that these transients are, for the most part, captured by the more detailed molecular theory developed in section III. This latter "contour-variable" theory incorporates the new constraint-release physics into a formalism that allows dependence of the chain orientation and stretch on the tube coordinate and also includes relaxation of chain ends by fluctuations. Section IV summarizes the results. In a subsequent paper, we will show that the new theory, in both simplified and contour-variable forms, can be extended in a natural way to account for polydispersity in molecular weight. The simplified theory for polydisperse systems collapses to the successful double-reptation formalism in the limit of linear viscoelasticity.

II. Simplified Model

II.A. Formulation. II.A.1. Chain-Stretching Model of Pearson et al. The starting point for our theory is the simplified version of the Marrucci−Grizzuti extension of the DE model developed by Pearson et al.[30] This theory contains three ingredients: an expression for the orientation tensor **S**, one for a scalar λ describing the stretch, and an expression for the stress tensor $\boldsymbol{\sigma}$ in terms of **S** and λ. These equations are

$$\mathbf{S} = \int_{-\infty}^{t} \frac{\mathrm{d}t'}{\tau_\mathrm{d}} \exp(-(t - t')/\tau_\mathrm{d})\mathbf{Q}(\mathbf{E}(t,t')) \tag{1}$$

$$\dot{\lambda} = \lambda\kappa{:}\mathbf{S} - \frac{1}{\tau_\mathrm{s}}(\lambda - 1) \tag{2}$$

$$\boldsymbol{\sigma} = 5G_\mathrm{N}^0\lambda^2\mathbf{S} \tag{3}$$

Equation 1 is the same expression for the orientation tensor **S** as in the original DE theory, with the minor difference that here we have included only the single, dominant, terminal relaxation time τ_d of that theory in the relaxation spectrum. The tensor $\mathbf{Q}(\mathbf{E}(t,t'))$ in eq 1 is the deformation-dependent "universal" tensor of Doi and Edwards defined by the deformation gradient history $\mathbf{E}(t,t')$:

$$\mathbf{Q} \equiv \left\langle \frac{\mathbf{E}\cdot\mathbf{u}'\mathbf{E}\cdot\mathbf{u}'}{|\mathbf{E}\cdot\mathbf{u}'|^2} \right\rangle_0$$

where $\mathbf{u}'$ is a unit vector distributed randomly over the unit sphere and $\langle\ \rangle$ represents an ensemble average over all $\mathbf{u}'$. The tensor **Q** is derived using the "independent alignment approximation" (IAA), which has a few flaws that are absent from the contour-variable theory in section III. G_N^0 is the entanglement plateau modulus.

Equations 1 and 3 with λ set to unity is just the DE equation, simplified by omission of all but the longest relaxation time. As described earlier, the only nonlinear rheological function that it describes well is the relaxation modulus at long times after a step strain. The Marrucci−Grizzuti extension of the DE equation corrects a major omission of the DE equation, namely, the stretching of the tube that occurs in flows faster than the inverse of the Rouse time for relaxation of the chain within the tube. While Doi and Edwards recognized the existence of the stretching process (and, indeed, discussed it at some length), for simplicity they assumed the Rouse relaxation to be very much faster than both reptation and the shearing rate, so that the tube always remains unstretched.

Tube stretching can be added to the DE theory in a simplied way by allowing λ in eq 3 to exceed unity and then including eq 2 in the DE's equation set. Equation 2 is the expression for the contour length of the primitive path, or "tube", describing the coarse-grained

path of the chain in its mesh of constraints. This length L is normalized by its equilibrium value L_0 so that $\lambda = L/L_0$. Equation 2 contains a "stretch" term $\lambda\kappa$:**S**, where κ is the velocity gradient tensor; this term leads to affine stretching of the molecule due to hydrodynamic drag on it from the mean-field friction of surrounding chains. The second term on the right side of eq 2 governs the relaxation of stretch, which is controlled by the longest Rouse time (or "stretch time") of the chain within the tube, τ_s. For strain rates much less than $1/\tau_s$, the inverse Rouse time, λ remains near unity and the original DE equation is recovered. For "fast" flows, i.e., flows for which $\dot{\gamma}\tau_s > 1$, the chain can stretch; i.e., λ can exceed unity.

Calculations with eqs 1−3, and with the more complete rigorous equation set proposed by Marrucci and Grizzuti, show that the inclusion of this chain-stretching process does improve the predictions of the theory for startup of fast shearing flows. The original DE equation predicts that, after the onset of shearing, there is an overshoot in the shear stress σ_{12}, but not in the first normal stress difference N_1. It also predicts that the strain at the overshoot in σ_{12} is insensitive to shear rate. These predictions are contradicted by experimental data which show large overshoots in both σ and N_1, which occur at strains that increase with increasing shear rate. The DEMG theory, on the other hand, predicts overshoots in both the shear stress and the first normal stress difference after startup of a fast shearing flow, and, furthermore, it predicts that the strains at the overshoot increase with increasing shear rate when $\dot{\gamma} > 1/\tau_s$, in agreement with the experiments.

Unfortunately, the improvement brought about by inclusion of tube stretch is limited to the features of the stress curves in startup of shearing, just described. When steady state is attained in shear, the predictions of the DEMG theory are just as bad as those of the DE theory. That is, the steady-state shear viscosity curve continues to show excessive shear thinning, with a power-law exponent of −0.5 for the shear stress at high shear rate. This may seem counterintuitive. One would think that at high shear rates the chain would be stretched, that is, λ would exceed unity, and the stress would then be increased, according to eq 3. Indeed, λ does increase from unity initially after startup of a fast shearing flow, and this produces the overshoot in N_1, which is missing from the DE theory. However, the shearing also rotates the chain into the flow direction, which decreases the shear component S_{12} of the orientation tensor **S**. This decreases the stretching term $\lambda\kappa$:**S** in eq 3, which in simple shearing is $\lambda\dot{\gamma}S_{12}$. Thus, as the shear rate $\dot{\gamma}$ increases, S_{12} at steady state decreases, and the product $\dot{\gamma}S_{12}$ at steady state is insensitive to shear rate. Hence, only during the transient period after startup is $\dot{\gamma}S_{12}$ large enough to drive tube stretching. Once S_{12} falls due to chain orientation, λ begins to drop back toward unity and the stress collapses back toward the DE value. (This lack of chain stretch in shear, but not in extension, plays an important role in a recent molecular theory for branched polymers by McLeish and Larson.[31])

A more generic problem with the DEMG theory is that even the transient chain-stretching effects that it does capture only occur at shear rates high enough that $\dot{\gamma}\tau_s \gtrsim 1$. For high-molecular-weight polymers, $\tau_d \gg \tau_s$, and there is a wide range of shear rates $\dot{\gamma}$ in the nonlinear regime for which $1/\tau_d < \dot{\gamma} < 1/\tau_s$. In this regime the flow is not fast enough to stretch chains, and the DEMG theory reduces to just the DE theory again. Since the predicted maximum in shear stress in the DE theory occurs at $\dot{\gamma} \approx 1/\tau_d$, it follows that for high molecular weights the DEMG theory, or any theory that merely adds tube stretch with a Rouse time constant to the DE theory, will continue to predict a maximum in the steady-state shear stress as a function of shear rate.

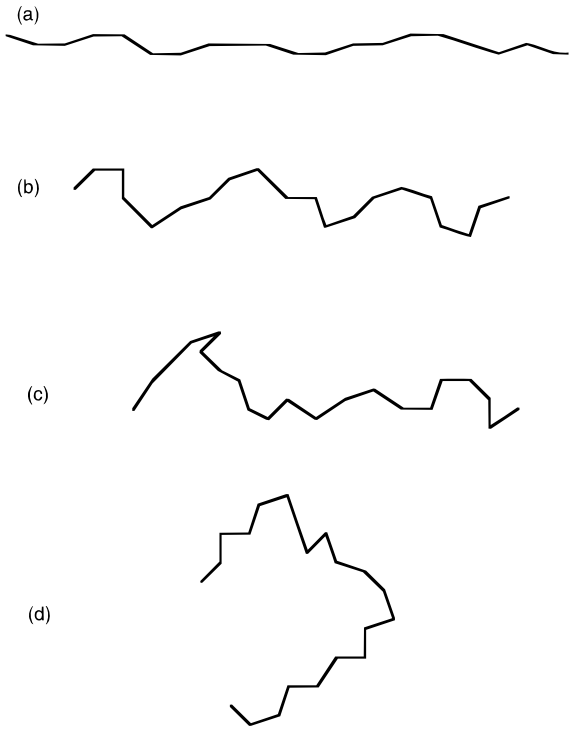

Figure 3. Relaxation of a portion of an initially highly deformed polymer chain.

What is needed, therefore, is a nonlinear relaxation mechanism that is active whenever $\dot{\gamma}\tau_d > 1$, that is, throughout the nonlinear regime, and not just in the regime where $\dot{\gamma}\tau_s > 1$. As discussed by Marrucci and Ianniruberto,[2,3] the most important mechanism missing from both the DE and DEMG theories is CCR. CCR is expected to occur when the mesh of constraints is flowing faster than the chain contained within it can relax, that is, when $\dot{\gamma}$ is larger than $1/\tau_d$. Incorporation of this effect into eqs 1−3 should then lead to a more successful model.

To incorporate CCR into the equations of Pearson et al., we must cope with this model's partitioning of stress into two contributions: the tube orientation **S** and the tube stretch λ. Of course, both stretch and "orientation" are manifestations of a single fundamental quantity, the bond-orientational order, which is the only source of stress in this model. Figure 3a−d depicts the relaxation of bond orientational order for a small portion of a polymer chain in the absence of flow. (A longer portion of this chain might have multiple folds but with bonds oriented along the same axis.) In Figure 4a−d, we superimpose onto this same sequence of chain configurations the constraints imposed by other chains, which we represent by small circles, and the tube in which the chain resides. The thin solid lines represent a tube whose diameter is that of the equilibrium chain, i.e., the entanglement spacing for the melt at rest. We suppose in Figure 4 that the constraints are fixed, so that the chain relaxes by retraction and reptation only.

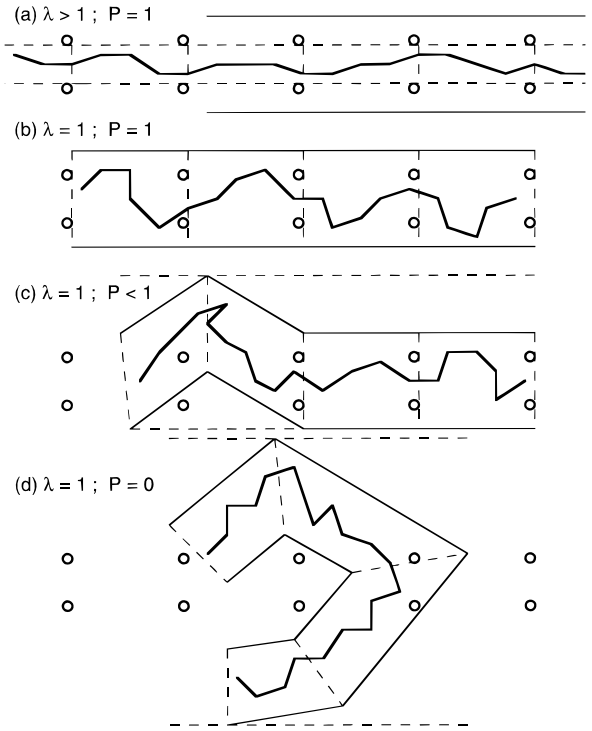

Figure 4. Relaxation of the chain in Figure 3 now viewed in terms of the tube model. The thin solid lines show the DE tube with constant diameter, and the small circles are constraints imposed by other chains. In parts a−c, the vertical dashed lines mark the tube segments. The horizontal dashed lines show an oriented tube whose diameter grows as the chain relaxes so as to encompass the relaxed chain. (a) The polymer chain is oriented ($P = 1$) and stretched ($\lambda > 1$), so that it occupies a tube that is longer and thinner than the equilibrium tube. (b) The chain stretch has relaxed ($\lambda = 1$), but the chain has not yet escaped the equilibrium oriented tube ($P = 1$). (c) The chain begins to escape the equilibrium tube, so the tube must reorient (solid lines) or its diameter must increase beyond the equilibrium diameter (dashed lines).

The relaxation of the stress tensor is derived from eq 3:

$$\boldsymbol{\sigma} = 5G_N^0\lambda^2(t)\,P(t)\mathbf{S}_0 \tag{4}$$

where $\mathbf{S}_0$ is the orientation tensor at the start of relaxation and $P(t)$ is the fraction of tube segments that remain oriented at time t.

In Figure 4a, the chain is stretched, $\lambda > 1$, which implies that it cannot explore its equilibrium tube, represented by the solid lines. The tube it actually explores on time scales that are short compared to the retraction time τ_s is shown by the dashed lines and is set by the lateral spacing of the entanglement constraints. Retraction occurs by Rouse processes, which wrinkle the chain to the maximum extent possible within the fixed constraints; see Figure 4b. On time scales longer than τ_s but much shorter than τ_d, the occupied tube therefore widens and it shortens its length to that of the equilibrium tube. Thus, the stretch λ decreases to unity, while the tube segmental orientation remains near unity. Further relaxation must occur by the much slower process of reptation. The effect of reptation, depicted in Figure 4c,d, is for the chain to escape the constraints and explore regions outside the equilibrium tube. This is represented within reptation theory by a reorientation of tube segments, i.e., a decrease in $P(t)$. If we were to insist on maintaining a fully oriented tube while still predicting the correct stress according to eq 4, we would have to allow the tube to shorten below its equilibrium length; i.e., λ would have to be allowed to decrease below unity, as the tube continues to widen, illustrated by dashed lines in Figure 4c,d. However, because the retraction process is governed by a time constant that is much shorter than that for reptation, λ can be kept from shrinking below unity and a clear distinction can be maintained between tube shrinkage and tube reorientation.

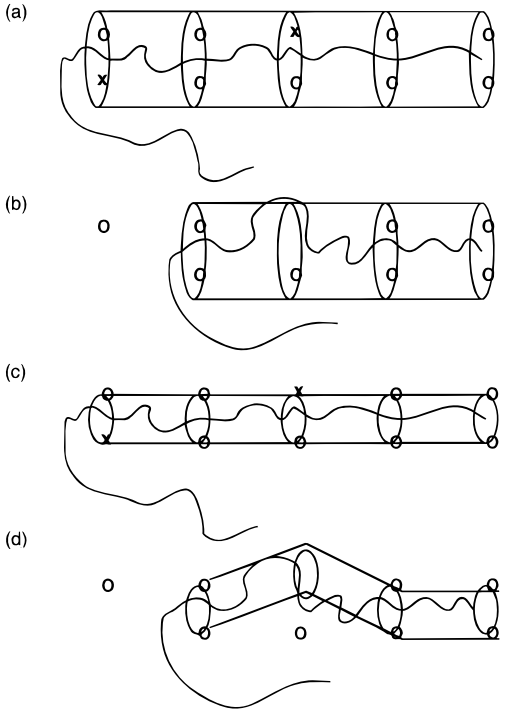

Figure 5. Two alternative descriptions of the effect of constraint release on the tube. (a and b) Two constraints (the x's) are removed by allowing the chain to relax. Since the tube does not fully occupy the tube (i.e., $\lambda > 1$), the chain relaxation results in a shorter, but still oriented, tube. (c and d) The same constraints are released and the chain relaxation is identical with that in parts a and b, but the chain fully occupies the tube ($\lambda = 1$) and so relaxation must be described in terms of tube reorientation rather than tube shrinkage.

When the constraints are not fixed, however, this separation of time scales no longer holds. Thus, consider a thought experiment in which the only means of relaxation of the test chain is by constraint release. Suppose some fraction of the constraints are released, and we consider time scales so short that the test chain can only execute localized Rouse motions, which permit reorientation of small pieces of the chain but do not allow either reptation or Rouse motion of the whole chain (which occur on time scales of τ_s or longer). Figure 5a−d shows two alternative descriptions of the effect of constraint release on the orientation and stretch of an initially stretched and oriented tube. In Figure 5a,b, the removal of two constraints (the x's) leads to tube shortening but no tube segment reorientation. In Figure 5c,d, the removal of the same constraints leads to tube segment reorientation but little or no tube shrinkage. Note that the chain configurations in Figure 5a,b are identical to those in Figure 5c,d; only the tube is different. Thus, *the stress and bond orientational order is the same in the two descriptions.*

Hence, when only constraint release is active, we have the luxury of two alternative descriptions of stress relaxation: we can reduce the primitive-path length or

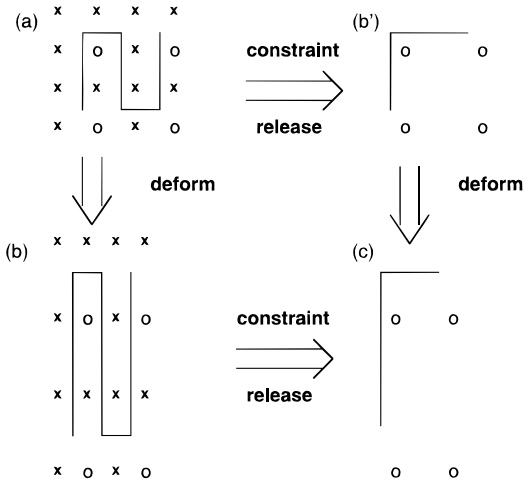

Figure 6. (a) Equilibrium primitive path of eight steps in a mesh of constraints suddenly deformed in a step strain (b). Then, $^3/_4$ of the constraints are removed (c), resulting in loss of $^3/_4$'s of the steps and a decrease in the length of the primitive path by a factor of 2. (b′) $^3/_4$ of the constraints are removed before the step deformation; the chain configuration after the step deformation is still given by part c.

reduce the tube-segment orientation. In the following, we show how each of these choices relaxes the same amount of stress when only constraint release occurs. We then show that the equivalency between tube stretch and tube orientation is sacrificed when reptation and retraction are turned on. We develop for that case a method of apportioning the effects of constraint release between tube stretch and tube orientation.

II.A.2. Effect of Constraint Release on the Tube Length. Let us first consider how constraint release can reduce the primitive-path length without changing the average primitive-path orientation. Figure 6a shows the primitive path of a chain lodged in a mesh containing both "permanent" constraints (the o's) and "transient" ones (the ×'s). This system is deformed in Figure 6b. When the transient constraints are removed in Figure 6c, the chain can explore a wider tube and the primitive path is therefore shortened. In Figure 6, the fraction of constraints removed is $^3/_4$. The amount of polymer in the given chain that is contained between two adjacent constraints is therefore increased on average by a factor of 4. Since, by definition, the chain executes a random walk between two adjacent constraints, the length of each step in the new primitive path must be increased by a factor of 2. There are only $^1/_4$ as many steps, however, so the total length of the primitive path is only half as long as before. Generalizing this argument, we find that the relationship between the length of the primitive path (L) and the number of constraints (n) is $L \propto \sqrt{n}$. If the number of entanglements changes because of constraint release, L will therefore change as

$$\frac{\mathrm{d}}{\mathrm{d}t}\ln(L(t)) = \frac{\dot{L}}{L} = \frac{1}{2}\frac{\dot{n}}{n} = -\frac{1}{2}k$$

where $k = -\dot{n}/n$ is the normalized rate of constraint release (i.e., $1/k$ is the lifetime of a constraint). Since $\lambda \equiv L/L_0$, we have

$$\dot{\lambda}_{\text{constraint release}} = -\frac{1}{2}k\lambda \qquad (5)$$

While this process of constraint release decreases the length of the primitive path, it has no tendency to change the average orientation of each step of the primitive path. To see this, we again return to our thought experiment, in which we have deformed the original tube affinely and then removed $^3/_4$ of the constraints, leaving the other constraints alone. If we had removed $^3/_4$ of the constraints first and then deformed the tube rather than the other way around, this would not have changed the resulting primitive path; see parts b′ and c of Figure 6. No matter what the lengths of the original steps in the primitive path are, these steps experience an affine rotation as a result of the deformation. Thus, in this description, removal of constraints following the step strain shortens the primitive path but does not change the average orientation of the steps in the path.

II.A.3. Effect of Constraint Release on Tube Orientation. We now describe the effects of constraint release in terms of tube segment reorientation. Returning to our thought experiment in which we remove $^3/_4$ of the constraints, we assume that this allows $^3/_4$ of the tube segments to reorient, with no change in stretch λ. Thus, the tube segment survival probability P is reduced by a factor of 4, and so is the bond orientational order and stress. This result is consistent with the tube-shortening picture; in that case removal of $^3/_4$ of the constraints led to a reduction of the stretch λ by a factor of 2. Since the stress tensor is proportional to λ^2 (see eq 4), tube shortening also reduces the stress 4-fold.

When only constraint release is occurring, at a rate k, the tube-survival probability $P(t)$ satisfies

$$\left.\frac{\partial P}{\partial t}\right|_{\text{constraint release}} = -kP \qquad (6)$$

Because $\boldsymbol{\sigma} \propto \lambda^2(t)\, P(t)$, eq 6, which describes constraint release in terms of tube reorientation, relaxes the same amount of stress as eq 5, which describes constraint release in terms of tube shortening.

II.A.4. Crossover between Tube Shortening and Tube Reorientation. When we turn reptation and retraction back on, the equivalence between tube shortening and tube reorientation cannot be maintained, at least within the formalism of Pearson et al., because of the large difference in the time scales between τ_s and τ_d. We must now enforce the condition that $\lambda \geq 1$. This can be done most simply by changing eq 5 to

$$\dot{\lambda}_{\text{constraint release}} = -\frac{1}{2}k(\lambda - 1) \qquad (7)$$

This implies that as tube shortening nears completion, constraint release is no longer manifested in tube shortening but must increasingly be manifested in tube reorientation. Thus, as we "switch off" tube shortening, we must "switch on" tube reorientation. The switching on of tube reorientation can be done by including a crossover or "switch" function $f(\lambda)$ in eq 6:

$$\left.\frac{\partial P}{\partial t}\right|_{\text{constraint release}} = -f(\lambda)\, kP \qquad (8)$$

Here $f(\lambda)$ must approach unity when λ nears unity, and $f(\lambda)$ approaches zero when λ is large. A simple, but ad hoc, form for the switch function is just an exponential, $f(\lambda) = \exp(-(\lambda - 1))$.

To derive a self-consistent formula for $f(\lambda)$, we return to our observation that, in the absence of other mechanisms of relaxation, constraint release should produce the same rate of stress relaxation whether it manifests itself as tube shortening or tube reorientation or, we might add, *some combination of the two*. We, therefore, derive $f(\lambda)$ by enforcing this equivalency on eqs 7 and 8. Thus, for a tube that is initially stretched to $\lambda = \lambda_0$ and oriented so that $\mathbf{S} = \mathbf{S}_0$, we consider in case 1 relaxation by tube reorientation only and in case 2 relaxation by a combination of tube reorientation and tube shortening, determined by the switch function $f(\lambda)$. For case 1, the stress relaxes as

$$\boldsymbol{\sigma}(t)|_1 = 5G_N^0 \lambda_0^2 e^{-kt} \mathbf{S}_0$$

In case 2, where we allow relaxation via both tube reorientation and tube shortening,

$$\boldsymbol{\sigma}(t)|_2 = 5G_N^0 \lambda^2(t)\, P(t)\, \mathbf{S}_0$$

where $\lambda(t)$ and $P(t)$ are the solutions of eqs 7 and 8:

$$\lambda - 1 = (\lambda_0 - 1) \exp(-kt/2)$$

$$P(t) = \exp\{-k\int_0^t f(\lambda(t'))\, dt'\}$$

Equating the stress in case 1 with the stress in case 2 yields a Volterra integral equation:

$$\lambda_0^2 e^{-kt} = \exp\{-k\int_0^t f(\lambda(t'))\, dt'\}[1 + (\lambda_0 - 1)e^{-kT/2}]^2$$

The solution to this equation is just $f(\lambda) = 1/\lambda$.

This derivation of the switch function, while better motivated than the ad hoc exponential $f(\lambda) = \exp(-(\lambda - 1))$, nevertheless depends on the expression we have chosen for $\dot{\lambda}_{\text{constraint release}}$ in eq 7. That is, the magnitude of $f(\lambda)$ for $\lambda > 1$ depends on how much of the constraint release is unaccounted for in eq 7. If we were to replace the right side of eq 7 by a function that more rapidly approaches $-{}^1/_2 k\lambda$ for $\lambda > 1$, then $f(\lambda)$ derived from the self-consistent argument would fall to zero more quickly when $\lambda > 1$. Fortunately, we find from calculations using both the "ad hoc" switch function $f(\lambda) = \exp(-(\lambda - 1))$ and the "self-consistent" function $f(\lambda) = 1/\lambda$ that the predictions of the theory are not very sensitive to the precise form of $f(\lambda)$, for shear rates where the theory is applicable, that is, for $\dot{\gamma}\tau_s < 10$.

II.A.5. Rate of Constraint Release due to Convection. The constraint-release process we are interested in here is that produced by convection of the chains surrounding the test chain. Not all convections or deformations will release constraints, however. In particular, if one rapidly deforms the polymer melt such that all chains deform affinely, then a test chain and its surrounding mesh will be deformed together, and all constraints on the test chain will survive. There will then be no constraint release. As recognized by Viovy et al.[38] and Marrucci and Ianniruberto,[2,5,39] constraint release will occur when the chains composing the mesh begin to undergo their *retraction* processes, i.e., when λ for the surrounding chains begins to decrease. For then, the constraints that the mesh chains impose on the test chain will begin to disappear. To be sure, new constraints will replace the old ones, but during this process, the interior portions of the test chain will have a chance to relax. Thus, the rate of convective constraint release, k, should be equal to the rate of convection of mesh of entanglements, $\boldsymbol{\kappa}:\mathbf{S}$, relative to the rate at which the test chain is stretched, $\dot{L}/L$. Hence,[2]

$$k = \left(\boldsymbol{\kappa}:\mathbf{S} - \frac{\dot{L}}{L}\right) \tag{9}$$

Note that when the test chain deforms affinely, $\dot{L}/L = \boldsymbol{\kappa}:\mathbf{S}$, and $k = 0$.

II.A.6. Constitutive Equation. By incorporating eq 7, the constraint-release contribution to $\dot{\lambda}$, into eq 2, and the contribution to chain reorientation, eq 8, into eq 1, using eq 9 for k, we obtain the set of equations for the simplified constraint-release model:

$$\frac{\partial P(t,t')}{\partial t} = -\frac{1}{\lambda^2 \tau_d} - f(\lambda)\left(\boldsymbol{\kappa}:\mathbf{S} - \frac{\dot{\lambda}}{\lambda}\right) \tag{10}$$

$$\mathbf{S} = \int_{-\infty}^{t} dt' \frac{\partial P(t,t')}{\partial t'} \mathbf{Q}(\mathbf{E}(t,t')) \tag{11}$$

$$\dot{\lambda} = \lambda \boldsymbol{\kappa}:\mathbf{S} - \frac{1}{\tau_s}(\lambda - 1) - \frac{1}{2}\left(\boldsymbol{\kappa}:\mathbf{S} - \frac{\dot{\lambda}}{\lambda}\right)(\lambda - 1) \tag{12}$$

$$\boldsymbol{\sigma} = 5G_N^0 \lambda^2 \mathbf{S} \tag{13}$$

The above equation set has two constraint-release terms; one is the last term in the equation for the tube survival probability, eq 10, and the other is the last term in the equation for stretch, eq 12. The first of these is important if the chain is not under tension. For then, the chain may be oriented, but it is able to explore the full volume of its tube; i.e., it has plenty of "slack". The release of constraints in this case can allow a slack chain segment to escape the tube and reorient; see Figure 5d. This is accounted for by the last term in eq 10. The other constraint-release term is dominant if the chain is under tension (i.e., $\lambda > 1$). Then, its primitive-path length is longer than equilibrium, and it cannot explore the entire volume of a tube whose diameter is that of the tube in the equilibrium melt; see Figure 5a. Thus, the chain has a shortage of slack, and the release of constraints will lead to a shortening of the length of the primitive path and a reduction in the stretch λ; see Figure 5b. This is accounted for in eq 12. Apart from these terms, eqs 10−13 are identical to eqs 1−3, with one additional, rather trivial, exception, namely, the incorporation of the factor of λ^2 multiplying τ_d in eq 10. This factor is included to make the equations of the simplified model consistent with those of the detailed molecular model described in section III; it accounts for the increase in the reptation time produced by the flow-induced lengthening of the molecule's primitive path. Since this only occurs when the chain is under tension ($\lambda > 1$) and under these conditions the dynamics are dominated by retraction and convective constraint release, the inclusion of this factor produces little difference in the model prediction but is included for consistency with the contour-variable model in section III.

We note that an alternative approach to account for constraint release is to consider the tube diameter to be time dependent, so that constraint release reduces bond-orientational order in only one way, namely, by expanding the tube diameter and thereby decreasing the

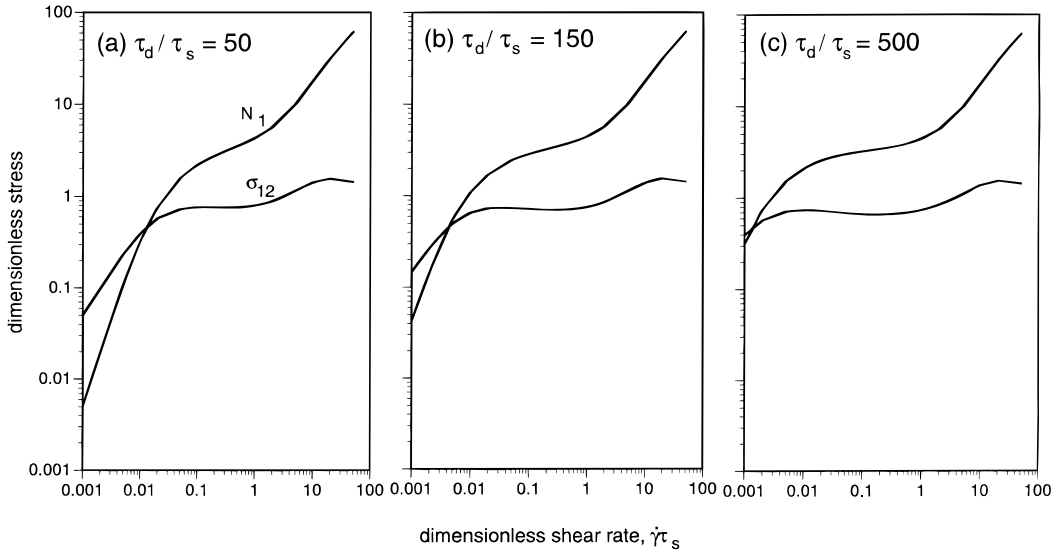

Figure 7. Steady-state values of the reduced shear stress σ_{12}/G_N^0 and first normal stress difference N_1/G_N^0 as functions of dimensionless shear rate $\dot{\gamma}\tau_s$ predicted by eqs 10−13 for $\tau_d/\tau_s =$ (a) 50, (b) 150, and (c) 500, where τ_d is the reptation time and τ_s is the Rouse retraction time. The self-consistent switch function, $f(\lambda) = 1/\lambda$, is used here and in Figures 9−13.

length of the primitive path. Such an approach has proved successful in describing linear relaxation in polydisperse melts of linear chains[7] and in relaxation of branched polymers,[15] for example. Marrucci and co-workers[5,32] and Wagner and co-workers[33,34] have also explored the possibility of using a variable tube diameter for the nonlinear rheology of linear chains, especially in step-shearing deformations. However, it appears to us that for an arbitrary nonlinear deformation history, a time-dependent tube diameter is conceptually and mathematically unwieldy, and so we prefer to ignore the tube diameter and instead allow constraint release to reduce either the length of the primitive path or the average orientation of each step of the path, depending on whether or not there is significant tube stretch.

Finally, we should add that our treatment only accounts for fast constraint-release processes that are associated with the largest contributions to the modulus. The slowest constraint-release process is governed by the Rouse time of the long chain in a "solvent" composed of the short chains, and hence its time scale is proportional to the reptation time of the short chains multiplied by the square of the number of entanglements in the long chain.[35−37] This long time scale is associated with a relatively small contribution to the modulus,[14] however, and is neglected here. Milner[14] discusses the conditions under which the this picture of constraint release is likely to be valid.

II.B. Predictions. In this paper, we will focus mainly on the predictions of the simplified model for various simple shearing histories, especially the flow histories for which the failings of the DE model are most notorious. Predictions for extensional and flows will be considered only briefly here. The theory contains only three parameters: the reptation time τ_d, the Rouse time τ_s governing the tube stretching/retraction process, and the plateau modulus G_N^0. These are the same parameters of the ordinary DE model and its extension by Marrucci and Grizzuti. In this section, we shall normalize all stresses by the plateau modulus G_N^0 and time and shear rate by the Rouse time τ_s. This leaves the ratio τ_d/τ_s as the only parameter of the model. This parameter is controlled by the polymer molecular weight (M) and concentration; theoretically, in the absence of fluctuation effects, one should have $\tau_d/\tau_s = 3N$, where for melts $N = M/M_e$ is the number of entanglements per chain, with M_e being the entanglement spacing.

II.B.1. Steady-State Shearing. In Figure 7a−c, we plot the steady-state values of the shear stress σ_{12} and the first normal stress difference N_1 for $\tau_d/\tau_s = 50$, 150, and 500 (corresponding to chains with 17, 50, and 170 entanglements per molecule), using the self-consistent switch function, $f(\lambda) = 1/\lambda$. As in the DE theory, in each case, there is the expected linear viscoelastic regime at low shear rates, $\dot{\gamma} \lesssim 1/\tau_d$, in which $\sigma_{12} \propto \dot{\gamma}$ and $N_1 \propto \dot{\gamma}^2$. The predictions of the theory at shear rates in excess of $1/\tau_d$ are very different from those of the DE or DEMG theories, however. Note that there is a nearly constant shear stress over a wide range of shear rates that extends from roughly $\dot{\gamma} \approx 1/\tau_d$ to $\dot{\gamma} \approx 10/\tau_s$; i.e., it becomes ever wider as τ_d/τ_s increases (i.e., as the molecular weight or concentration increases). The shear stress is not exactly constant in this regime but decreases very slightly with increasing shear rates in the range $5/\tau_d \lesssim \dot{\gamma} \lesssim 0.5/\tau_s$. The minimum value of η is only about 10% less than the value at the local maximum near $\dot{\gamma} \approx 1/\tau_d$. Hence, the behavior predicted by the new model is quite different, and much more realistic, compared to that of the DE model, for which $\sigma_{12} \propto \dot{\gamma}^{-0.5}$ at shear rates above $1/\tau_d$.

The predictions obtained from the ad hoc exponential switch function $f(\lambda) = \exp(-(\lambda))$ are shown in Figure 8a−c. They are very similar to the predictions shown in Figure 7a−c, except for high $\dot{\gamma}\tau_s \gtrsim 10$, where the stresses for the self-consistent switch function are somewhat higher than those for the ad hoc switch function. In this range of very high shear rates, however, the behavior ought to be strongly influenced by higher-mode Rouse-like relaxation times that are shorter than the longest Rouse mode. Since such relaxation mechanisms are omitted from the theory, we do not consider the predictions of the model in to be valid in this regime anyway. In what follows, calculations with the simplified model are presented only for the self-consistent switch function $f(\lambda) = 1/\lambda$. Similar results were obtained with the ad hoc switch function.

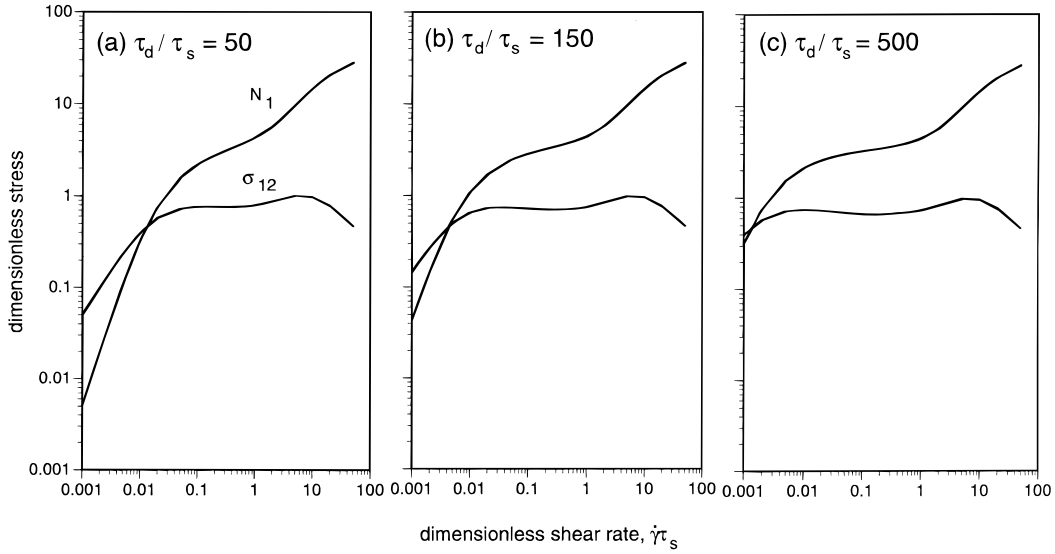

Figure 8. Same as Figure 7, except that the ad hoc switch function, $f(\lambda) = \exp(-(\lambda - 1)$, is used.

Compare now the predictions in Figure 7a with the measurements in Figure 1a on a polystyrene solution with a similar entanglement density, i.e., a similar value of $\tau_d/\tau_s \approx 50$. The behaviors of the predicted shear stress and first normal stress difference are quite similar to the measured responses. The measured curves have slightly higher slopes than those predicted, but we shall see later that even these disparities are greatly reduced when primitive-path-length fluctuations are accounted for in section III.B.

While the behavior in the regime $\dot{\gamma} < 1/\tau_d$ is controlled by reptation and is the same as that predicted by the original DE theory and the behavior at $\dot{\gamma} > 1/\tau_s$ is influenced by tube stretching, CCR introduces a new "intermediate" regime between the reptation regime ($\dot{\gamma} < 1/\tau_d$) and the chain-stretching regime ($\dot{\gamma} > 1/\tau_s$). Stress relaxation in this intermediate regime ($1/\tau_d < \dot{\gamma} \lesssim 1/\tau_s$) *is dominated by constraint release*; both chain stretching and ordinary reptative relaxation are virtually irrelevant. The relaxation process in the intermediate regime is described and contrasted with that of ordinary reptation in appendix A. For $\tau_d/\tau_s \gg 1$, the constraint-release regime is very broad, and in the middle of the regime one can neglect entirely both reptation and chain stretching. In that case, which is analyzed in appendix B, one finds that both the shear stress σ_{12} and the first normal stress difference N_1 approach constant values, $\sigma_{12}/G_N^0 = 0.615$ and $N_1/\sigma_{12} = 5.44$. This intermediate shear-rate regime also appears in the theory of Marrucci and Ianniruberto;[5] in fact, the shear-stress curve for $\beta = 1$ in their theory is identical to ours in the limit of very large τ_d/τ_s, with $\dot{\gamma}\tau_s \lesssim 1$.

We compare the shear viscosity curves for the three different entanglement densities in Figure 9. As a basis for comparison, we have assumed that the curves correspond to melts of different molecular weight and that the reptation scaling $\tau_d \propto M^3$ and $\tau_s \propto M^2$ applies. Thus, we take $\tau_s \propto (\tau_d/\tau_s)^2$. Hence, to obtain Figure 9, the shear-rate axes of parts b and c of Figure 7 are rescaled by factors of $(150/50)^2$ and $(500/50)^2$, respectively, relative to that for Figure 7a. Since the viscosity is the stress divided by the shear rate, the viscosities must be rescaled by similar factors. Note that all the viscosities nearly collapse to a common curve at high shear rates, similar to the behavior observed in experiments.

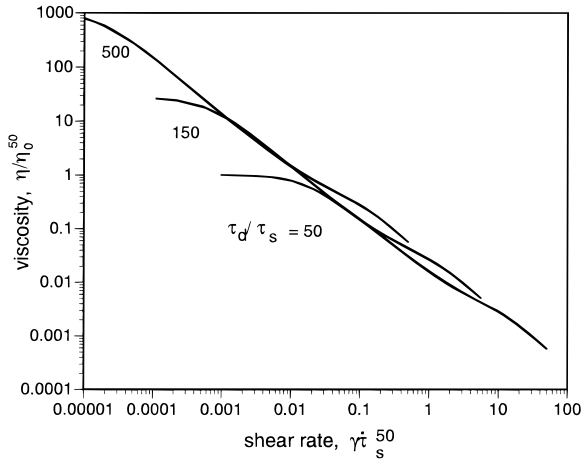

Figure 9. Steady-state reduced shear viscosity versus shear rate for $\tau_d/\tau_s = 50$, 150, and 500, corresponding to successively higher molecular weights of a melt predicted by eqs 10−13. The curves are scaled using the assumptions that $\tau_s \propto M^2$ and $\tau_d \propto M^3$, where M is the chain's molecular weight; thus, M is proportional to τ_d/τ_s.

The realistic behavior of the theory is a consequence of its accurate predictions of the steady-state extinction angle χ and the tube stretch λ as functions of shear rate. These are shown in Figure 10a,b for the case $\tau_d/\tau_s = 50$. Note that χ is predicted to decrease at first rapidly with increasing shear rate and then much more slowly. This prediction compares very favorably with the measured χ values in Figure 1b for an entangled polystyrene solution. As expected, the stretch λ remains nearly relaxed at unity as long as the shear rate is less than the inverse Rouse relaxation time $1/\tau_s$. However, once $\dot{\gamma}\tau_s$ exceeds unity, λ begins to increase modestly, up to around 1.7 at $\dot{\gamma}\tau_s = 10$. The predicted behaviors of both χ and λ contrast strongly with the predictions of the original DE model and of the DEMG model. Both these models predict a continued rapid drop in χ at shear rates much above $1/\tau_d$. This rapid drop in χ means that the tube segments rotate nearly completely into the flow direction, where the shear flow can no longer exert much drag, and the chain cannot therefore sustain stretch.

To be more precise, the term in eq 12 that drives tube stretching is $\kappa:\mathbf{S} = \dot{\gamma}S_{12}$. A low value of the extinction angle χ implies that S_{12} is small; hence, the chain will

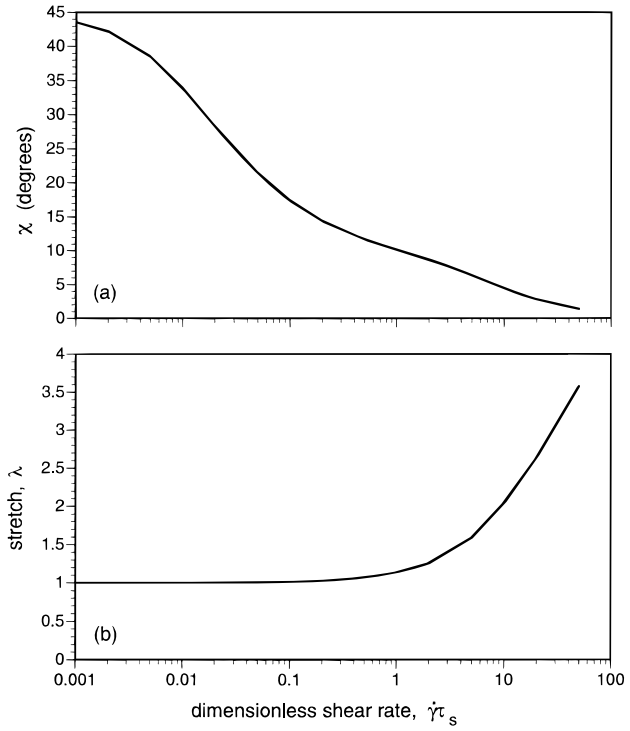

Figure 10. Steady-state values of (a) extinction angle χ and (b) stretch λ as functions of dimensionless shear rate $\dot{\gamma}\tau_s$ for $\tau_d/\tau_s = 50$, predicted by eqs 10−13 for $\tau_d/\tau_s = 50$.

not be able to maintain a stretched configuration. When the influence of convective constraint release is incorporated into the equation for the orientation tensor via eqs 10 and 11, however, χ does not decrease so rapidly and λ can begin to increase when $\dot{\gamma} > 1/\tau_s$. This effect is delicately balanced, so that runaway tube stretching does not occur for $\dot{\gamma}\tau_s > 1$. When the chain begins to stretch significantly, the tube-segment reorientation mechanism is attenuated by the suppression of the constraint-release term (last term) via the switch function in eq 10. When this happens, χ will begin to decrease, and this will lead to a shrinkage of the chain length via eq 12. If the chain tries to shrink too much, however, the chain-segment reorientation process is reactivated, and χ begins to increase again, which arrests the decrease in λ via eq 12. Thus, the retreat of the chain ends back into the tube does not turn into a complete rout, which would lead to catastrophic shear thinning, as occurs in the DE and DEMG models. Stretch and orientation therefore balance themselves in such a way that a region of nearly constant shear stress is obtained over a range of shear rates that extends up to $\dot{\gamma}\tau_s = 10$.

II.B.2. Startup and Cessation of Shearing. Figure 11 shows the growth of the shear stress σ_{12} and first normal stress difference N_1 after startup of steady shearing at $\dot{\gamma}\tau_s = 1$, 2, 5, and 10, the last three of which are high enough to induce significant tube stretching. Note that, for $\dot{\gamma}\tau_s \gtrsim 2$, both σ_{12} and N_1 show transient overshoots; at each $\dot{\gamma}\tau_s$ the overshoot in N_1 occurs at a higher shear strain than that for the shear stress. These overshoots, and the strains at which they occur as functions of $\dot{\gamma}\tau_s$, are in qualitative agreement with experimental data.[19] The overshoots are also predicted by the DEMG theory and occur in the new model for the same reason they do in the old one: the large driving force for tube stretch induced by onset of fast flow

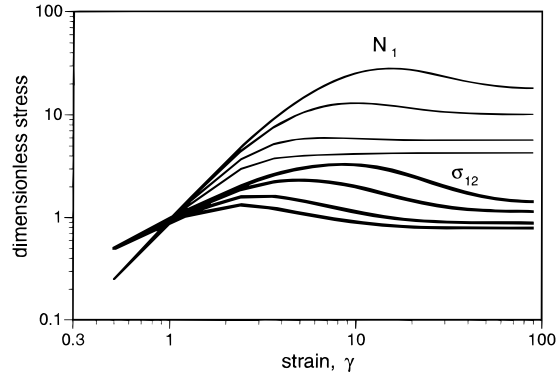

Figure 11. Dimensionless shear stress σ_{12}/G_N^0 (thick lines) and first normal stress difference N_1/G_N^0 (thin lines) as functions of strain γ after startup of steady shearing at high dimensionless shear rates $\dot{\gamma}\tau_s = 1$, 2, 5, and 10, predicted by eqs 10−13 for $\tau_d/\tau_s = 50$. As $\dot{\gamma}\tau_s$ increases, the maxima in σ_{12} and N_1 become more pronounced and shift to higher strains.

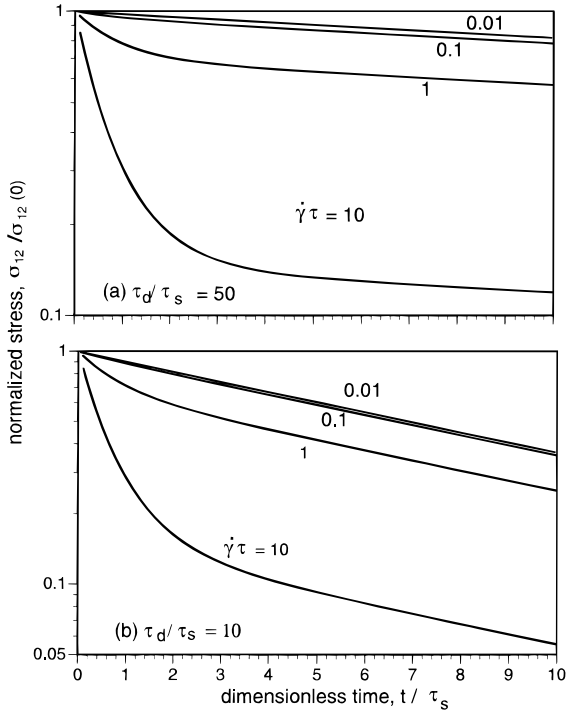

Figure 12. Relaxation of shear stress σ_{12} reduced by its value $\sigma_{12}^{ss} = \sigma_{12}(0)$ at steady state as a function of dimensionless time t/τ_s after cessation of steady-state shear, for prior dimensionless shear rates $\dot{\gamma}_0\tau_s$ of 0.01, 0.1, 1, and 10, predicted by eqs 10−13 for (a) $\tau_d/\tau_s = 50$ and (b) $\tau_d/\tau_s = 10$.

diminishes once the chains become oriented toward the flow direction, i.e., once χ becomes low.

Figure 12 shows the relaxation of the shear stress, normalized by its initial value, after cessation of steady shearing for $\tau_d/\tau_s = 50$ and 10. These predictions show that when the shear rate is much less than $1/\tau_s$, the stress relaxation is independent of the steady shear rate and is controlled by the reptation time τ_d. At higher shear rates, however, the rate of relaxation is initially faster by a factor that is roughly proportional to the previous shear rate $\dot{\gamma}$. Later in the relaxation process, at $t > \tau_s$, the relaxation rate reverts back toward a rate governed by τ_d. This behavior, which is observed in experiments,[27,28] is a consequence of relaxation of chain stretch and its effect on the constraint-release term in eq 10. Note that this accelerated relaxation only begins to occur when the tube is stretched, i.e., $\lambda > 1$. If $\dot{\gamma}\tau_s <$

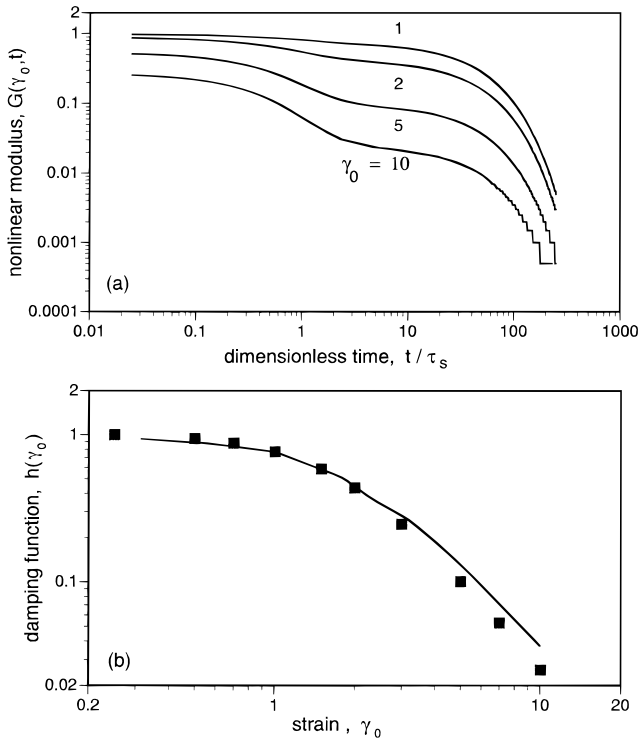

Figure 13. (a) Relaxation of dimensionless shear modulus $G(\gamma_0,t) \equiv \sigma_{12}/(G_N^0\gamma_0)$ as a function of dimensionless time t/τ_s, after step shear strains of magnitudes γ_0 of 1, 2, 5, and 10, from top to bottom, predicted by eqs 10−13 for $\tau_d/\tau_s = 50$. (b) The damping function $h(\gamma_0) \equiv G(\gamma_0,t=10\tau_s)/G(\gamma_0=0.25,t=10\tau_s)$ is given by the symbols, and the DE theory without the independent alignment approximation is given by the line.

1, on the other hand, after cessation of shearing, $\dot{\gamma}$ and $\dot{\lambda}$ are both zero, and CCR is therefore shut off immediately. Hence, for $\dot{\gamma}\tau_s < 1$, the relaxation time τ immediately reverts to equilibrium value τ_d.

II.B.3. Step Shear. Figure 13a shows the predictions the model makes for the nonlinear modulus $G(\gamma_0,t) \equiv \sigma_{12}/\gamma_0$ describing relaxation after step shears of various magnitudes γ_0. The results are qualitatively similar to experimental data, for example, the data of Osaki and co-workers.[18,40] At short times, $t/\tau_s \ll 1$, the failure of the moduli to coalesce onto a common line is largely due to the independent alignment approximation (IAA). Marrucci and Ianniruberto[39] have noted that CCR, if applied naively to the problem of relaxation after a step strain, produces overly severe stress relaxation. This is because CCR occurs after the step shear as a result of the retraction of chains surrounding a given chain. The release of these constraints relaxes stress and therefore leads to a smaller stress than that predicted by the DE theory. However, the DE theory already predicts this stress accurately; in fact, this one success of the theory is largely responsible for the wide interest and acceptance of the DE model as at least a starting point for understanding the nonlinear rheology of entangled polymer melts and solutions.

Thus, incorporation of CCR into the DE reptation theory cannot improve the theory's already excellent prediction of the step-strain response but might well degrade it. An improvement in the predictions of steady-shear-flow behavior by incorporation of CCR would be but a Pyrrhic victory if this addition to the theory should destroy its ability to predict accurately the response in a step strain. Calculations with our equations show, however, that any such degradation in the predictions of the step-strain response is small; Figure 13b (symbols) shows the nonlinear "damping function" extracted from the curves in Figure 13a by plotting the "plateau modulus" $G(\gamma_0,t/\tau_s = 10)$ normalized by its low strain ($\gamma_0 = 0.25$) value at a fixed time $t/\tau_s = 10$ against step-shear strain γ_0. The results are similar to the DE damping function, which agrees well with that measured by Osaki and co-workers for polystyrene solutions in the moderately entangled regime. The largest deviation from the DE damping function occurs at large strains; this deviation is toward an increase in strain softening. CCR produces a multiplicative correction, $h_{CR}(\gamma_0)$, to the DE damping function h_{DE}; i.e., $h(\gamma_0) = h_{DE}(\gamma_0) \times h_{CR}(\gamma_0)$. At high strains and for large τ_d/τ_s, h_{CR} approaches an asymptotic value of $\exp(-0.5963) = 0.5508$ for the ad hoc switch function and $\exp(-1) = 0.3679$ for the self-consistent one; see eq C17 in appendix C.

It is difficult to assess whether or not this modest deviation of $h(\gamma_0)$ from $h_{DE}(\gamma_0)$ should be a cause for concern. Agreement with the DE damping function is good for monodisperse melts and solutions with $N = 20-50$ entanglements/molecule.[41] Monodisperse melts and solutions with considerably fewer than $N = 20$ entanglements/molecule show upward departures in $h(\gamma_0)$ from the DE theory,[42] while those for which $N \geq 50$ show large downward departures,[43−46] due to either slip[47] or strain inhomogeneities.[48] In addition, in the contour-variable model to be described below, the deviation from the DE damping function appears to be even less than that in the simple model discussed here. Thus, the small departure from the DE damping function at high strain is probably not significant.

The reason CCR does not produce a much larger decrease in the damping function is because the chain reorientation mechanism in eq 10 is suppressed by the switch function $f(\lambda) \rightarrow 0$ when the chains are highly stretched immediately after the step strain. Thus, convective constraint produces significant chain reorientation only when the chains *both* are retracting relative to the flow *and* are not highly stretched. Just after a step strain, during the early stages of chain retraction, only the first condition is met, while near the end of chain retraction only the second condition is met. Hence, both conditions are met simultaneously only to a small degree, and little chain reorientation occurs during chain retraction. Thus, when chain retraction nears completion ($\lambda \rightarrow 1$), the tube segments that remain are nearly as highly oriented as they were at the start of retraction.

II.B.4. Steady-State Extension. The predictions of the model in extensional flows are quite similar to those of the original DEMG model. For extension, unlike shear, CCR has a quantitative, but not qualitative, effect on the predictions, because in extension the extinction angle does not vary with shear rate, and so there is no delicate balance between chain stretch and extinction angle, as there is in shear. At steady state, the model shows three regimes of extension rate: a low rate, $\dot{\epsilon} < 1/\tau_d$, where the viscosity is rate independent and equal to the Trouton value; an intermediate regime, $1/\tau_d \ll \dot{\epsilon} \ll 1/\tau_s$, in which the extensional stress is constant and equal to the value $3.04G_N^0$; and a high extension-rate region, $\dot{\epsilon} \gtrsim 1/\tau_s$, where the viscosity increases with increasing strain rate. The behavior in the latter two regimes is analyzed at the end of appendix B. In the second regime, the viscosity is extension thinning, scaling as $\dot{\epsilon}^{-1}$. In the third regime, the extensional viscosity shows a runaway extension thick-

ening, becoming singular when $\dot{\epsilon} = 2/\tau_s$. The singular behavior is a consequence of the dominance of Rouse-like behavior for $\dot{\epsilon} > 1$. For real polymers, finite extensibility of the chain will cause the strain thickening to saturate at a finite value of the viscosity. Extensional flow data on monodisperse, linear polymers are still lacking, so these unusual predictions, which are also present in the DEMG model, have not yet been tested.

In summary, we have shown that this new, simplified model for constraint release is in excellent qualitative, and, to some extent, quantitative, agreement with many of the shear-flow measurements for which earlier reptation models fail, including measurements 1−4 described in the Introduction. The simple model does not, however, alleviate failure number 5; transients in χ after a stepup or stepdown in shear rate remain monotonic in the simple constraint-release model presented above. However, we will now show that this limitation of the simple model is lifted when the new constraint-release physics are incorporated into a more complete model that includes the contour-length-variable and fluctuation effects.

III. Contour-Variable Model

III.A. Formulation. We here present our contour-variable model incorporating CCR into the DEMG equations.[19,20] These equations contain functions of the primitive-path contour length variable s, which runs from $-L/2$ to $L/2$, i.e., from one end of the primitive path to the other. Since the primitive path can stretch, L may be larger than the equilibrium chain length L_0. Thus, we define the function $s(s_0)$ as a mapping $s_0 \rightarrow s$ of the tube coordinate s_0 that runs along the relaxed tube from $-L/2$ to $L_0/2$ to the coordinate s of the stretched tube that runs from $-L/2$ to $L/2$.

The tube survival probability function $G(s,t,t')$ is a function of s as well as of the present time t and past time t'; it is the probability that a tube segment located at s_0 at time t' survives until time t.

The DEMG theory contains four major equations, one for the tube survival probability function $G(s,t,t')$, one for the orientation tensor $\mathbf{S}(s,t)$, another for the stretch function $s(s_0,t)$, and a fourth for the stress tensor $\boldsymbol{\sigma}(t)$ in terms of $G(s,t,t')$ and $\mathbf{S}(s,t)$. These equations are the counterparts to eqs 10−13 in the simple model. Another equation is required to define variables that appear in the main equations. The equations we propose for the DEMG equations with CCR are

$$\frac{\partial G(s,t,t')}{\partial t} = D\frac{\partial^2 G}{\partial s^2} - \langle v\rangle \frac{\partial G}{\partial s} + f\left(\frac{\partial s}{\partial s_0}\right)\left[\frac{2}{L(t)}(\dot{s} - \langle v\rangle)_{s=L/2}\right]G \quad (14)$$

$$\mathbf{S}(s,t) = \int_{-\infty}^{t} dt' \frac{\partial G}{\partial t'}\hat{\mathbf{Q}}(\mathbf{E}(t,t')) \quad (15)$$

$$\frac{\partial s(s_0,t)}{\partial t} = \langle v\rangle + 3ND\frac{\partial^2 s}{\partial_0{}^2} - \frac{1}{2}\left[\frac{2}{L(t)}(\langle v\rangle - \dot{s})_{s=L/2}\right](s - s_0) \quad (16)$$

$$\boldsymbol{\sigma}(t) = \frac{15}{4}G_N^0\frac{1}{L_0}\int_{-L_0/2}^{L_0/2} ds_0\, \mathbf{S}(s_0,t)\left(\frac{\partial s}{\partial s_0}\right)^2 \quad (17)$$

where $\langle v\rangle$ is given by

$$\langle v(s,t)\rangle = \kappa : \int_0^s \mathbf{S}(s',t)\, ds' \quad (18)$$

The boundary and initial conditions are

$$G(s,t,t') = 0 \text{ at } s = -L/2,\ L/2; \quad G(s,t,t') = 1 \text{ at } t = t';$$
$$\frac{\partial s(s_0,t)}{\partial s_0} = 1 \text{ at } s = -L/2,\ L/2; \quad \frac{\partial s(s_0,t)}{\partial s_0} = 1 \text{ at } t = 0$$

In eqs 14−17, we have for compactness suppressed the dependencies of the various functions on s, s_0, t, and t', except on the left side of the equations. We have also defined the substantial time derivative of s as $\dot{s}$. The tensor $\hat{\mathbf{Q}}$ in eq 15 is the DE strain tensor *without* the independent alignment approximation:

$$\hat{\mathbf{Q}} \equiv \left\langle \frac{\mathbf{E}\cdot\mathbf{u}'\mathbf{E}\cdot\mathbf{u}'}{|\mathbf{E}\cdot\mathbf{u}'|}\right\rangle_0 \frac{1}{\langle|\mathbf{E}\cdot\mathbf{u}'|\rangle_0}$$

In eqs 14 and 16, the curvilinear diffusion coefficient D is related to the reptation time by $\tau_d = L_0{}^2/\pi^2 D$. As earlier, the Rouse stretch time is given by $\tau_s = \tau_d/3N$, where $N = M/M_e$ is the number of entanglements per chain. The tube velocity $v(s,t)$ is the velocity of the mesh of constraints surrounding tube segment s relative to the center of the chain at $s = 0$; it is preaveraged over all surrounding chains and is therefore given as $\langle v(s,t)\rangle$, which can be computed from the velocity gradient tensor κ via eq 18.

The last term in eq 14 describes the effect of CCR on the orientation probability function. It is the natural extension of the last term in eq 10 from the simplified model, where the function $f(\partial s/\partial s_0)$ is the "switch function". As we showed earlier, the results are not very sensitive to the switch function for $\dot{\gamma}\tau_s \lesssim 10$. For the calculations in this section, we will use the ad hoc switch function $f = \exp(-(\partial s/\partial s_0))$. The last term in eq 16 incorporates CCR into the equation for tube stretch; again it is the analogue of the corresponding term in eq 12. Both these terms are evaluated at the tube end $s = L/2$, because constraints are released only when the end of a neighboring chain is convected through the tube of the test chain. Also, only one end need be considered; the effect of the other is included automatically by symmetry. (The factor of 2 in the constraint-release terms of eqs 14 and 16 accounts for the two chain ends if the whole chain is considered and accounts for the factor of 2 which must divide L if only a half chain with one chain end is considered.) The other terms are equivalent to those found in Pearson et al.[19] and Mead and Leal[20] and are discussed there. These equations will also be discussed in more detail in a forthcoming publication.

Finally, we note that this theory readily admits inclusion of fluctuations in the length of the primitive path. As discussed by de Gennes,[49] Doi and Kuzuu,[50] Pearson and Helfand,[51] and Doi and Edwards,[18] the rate of relaxation of a chain segment due to primitive-path-length fluctuations increases exponentially with distance from the chain ends. These fluctuations, also called "breathing" or "concertina" modes, involve migration of the chain ends into the tube, thus temporarily creating a higher-than-average density of chain slack along the primitive path. When the chain end moves outward again, it is free to follow a path different from the original one; the portion of the tube vacated during

the inward breathing motion is forgotten, and the stress associated with it is relaxed. Deep fluctuations, which evacuate large portions of the tube, are exponentially less probable than shallow ones. Thus, this relaxation process adds a term $-G(s,t,t')/\tau_\xi(s_0)$ to the right side of eq 14, where the relaxation time τ_ξ is an exponential function of the relative distance ξ from the chain end. That is

$$\tau_\xi(s_0) \equiv \tau_0 \exp\left(\nu \frac{N}{2}\xi^2\right) \tag{19}$$

with $\xi \equiv 1 - 2|s(s_0)|/L$. For the time constant τ_0 we use the Rouse time of half the chain; i.e., $\tau_0 = \tau_s/4$. A more accurate prefactor, one which depends on ξ, has been derived by Milner and McLeish.[52] The exponent ν was estimated to be 1.5 by Doi and Kuzuu.[50] (The precise value of ν depends on the convention used in the definition of the entanglement molecular weight; for the convention of Fetters et al.[53] used here, $\nu = 1.5$. For the convention used in Ball and McLeish,[15] a value $^5/_4$ times larger is appropriate; namely, $\nu = {}^{15}/_8$.) Ball and McLeish[15] showed that fluctuation-induced constraint release modifies eq 19 by addition of a cubic term in ξ inside the exponential. This cubic term weakens the dependence of τ_ξ on ξ, but this effect is small for small ξ, i.e., for the "shallow" fluctuation modes that have the greatest influence in the present context. Therefore, here it suffices to retain only the quadratic term.

Thus, the contour-variable theory proposed here includes reptation as proposed by de Gennes, chain retraction described by Doi and Edwards and Marrucci and Grizutti, fluctuation effects borrowed from de Gennes, Kuzuu and Doi, and Ball and McLeish, and CCR suggested by Marrucci and Ianniruberto. Three of these four mechanisms are included in eqs 14−18, and the fourth, the fluctuation effect, is added by replacing eq 14 by

$$\frac{\partial G(s,t,t')}{\partial t} = D\frac{\partial^2 G}{\partial s^2} - \langle v\rangle \frac{\partial G}{\partial s} + f\left(\frac{\partial s}{\partial s_0}\right)\left[\frac{2}{L(t)}(\dot{s} - \langle v\rangle)_{s=L/2}\right]G - \frac{G}{\tau_\xi(s_0)} \tag{20}$$

Equations 14−18, which neglect fluctuation effects, or eqs 15−20, which include them, are solved by finite differencing and numerical integration, as described elsewhere.[20,21] The time step required in the integration is set by the fastest relaxation process, which for eqs 15−20 is given by eq 19 with $\xi = 0$. Since time steps this small would greatly slow down the integration of the equations, we obtain solutions to eq 20 by first solving the equation in the absence of fluctuation effects (i.e., with the last term dropped), and then after each time step, we multiply this solution for $G(s,t,t')$ by $\exp(-\Delta t/\tau_\xi)$, where Δt is the time step. This procedure gives rigorously correct results for chain segments well away from the chain ends, where $\Delta t/\tau_\xi \ll 1$, and was found by variation of the time-step size to give accurate results in general, at least for the quantities computed here.

III.B. Predictions. The results reported in this section will focus on a single ratio of reptation to Rouse times, $\tau_d/\tau_s = 50$, corresponding to $N \approx 17$ entanglements per chain. This matches the conditions of the experimental results shown in Figures 1 and 2. In this section, we will make the shear rate and time dimensionless using the more conventional reptation time τ_d, rather than the Rouse time τ_s, which was convenient in comparing results for different numbers of entanglements in section II.

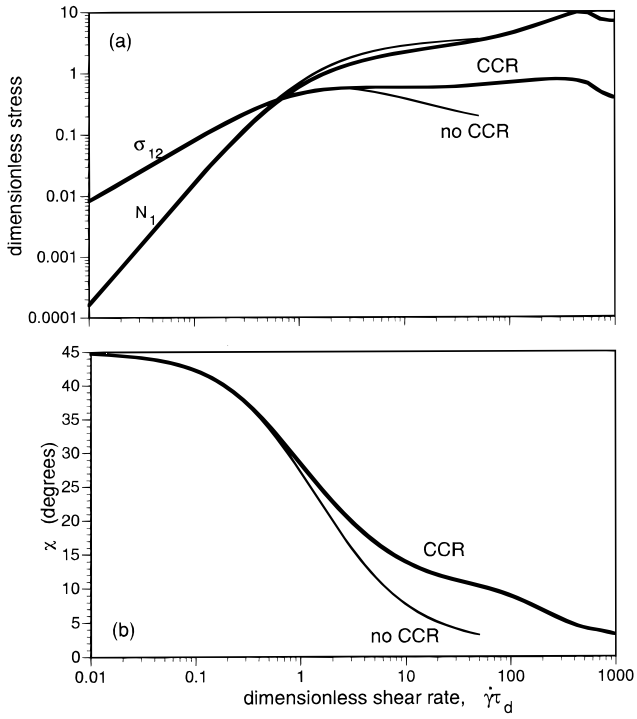

Figure 14. (a) Steady-state dimensionless shear stress σ_{12}/G_N^0 and first normal stress difference N_1/G_N^0 and (b) extinction angle χ as functions of shear rate $\dot{\gamma}$ made dimensionless by the reptation time τ_d. The thick lines are from eqs 14−18, for the contour-variable model including CCR but without fluctuation effects. The thin lines are the predictions of the DEMG theory, which neglects CCR. In all cases, in this figure and Figures 15−17, there are $N = 50/3$ entanglements per molecule (thus, $\tau_d = 50\tau_s$), and the ad hoc switch function, $f(\lambda) = \exp(-(\lambda - 1))$, is used.

Figure 14a shows the shear-rate dependence of the shear stress and first normal stress difference as functions of Weissenberg number $Wi \equiv \dot{\gamma}\tau_d$ for the theory without fluctuations; Figure 14b shows the corresponding plot for the extinction angle χ. For comparison, results from the DEMG theory, which neglects both fluctuations and CCR, are also shown. Agreement of the predictions of the contour-variable model with the experimental data in Figure 1 is very good. It is clear from Figure 14 that omission of CCR leads to an excessively steep decrease in χ with increasing shear rate $\dot{\gamma}$ and, consequently, to a decreasing shear stress as a function of $\dot{\gamma}$ at high shear rate.

With CCR, the predictions of the contour-variable model are very similar to those of the simplified model described in section II; compare Figure 14 with Figure 7. The predictions are similar because the tube survival function $G(s,t,t')$ in the former model is nearly uniform, except at shallow boundary layers near the free ends of the molecule. These boundary layers are much shallower when CCR is present than when it is absent, as discussed in appendix A.

Parts a and b of Figure 15 show the effect on the steady-state shear stress and the viscosity of including fluctuations via the last term of eq 20. The fluctuations reduce the zero-shear viscosity and increase the slope of the stress versus shear rate curve so that *the shear stress becomes a monotonic function of shear rate.*

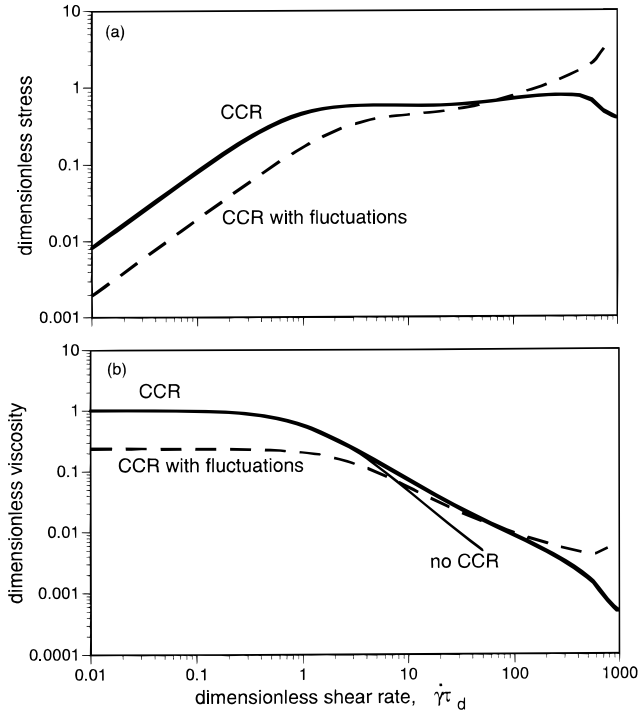

Figure 15. (a) Dimensionless steady-state shear stress and (b) dimensionless shear viscosity as functions of $\dot{\gamma}\tau_d$ predicted by the contour-variable model, both without fluctuation effects (thick solid lines: eqs 14−18) and with fluctuation effects (dashed lines: eqs 15−20). The prediction of the DEMG theory in part b is given by the thin solid line.

Consequently, the shear thinning is reduced. The increase in the slope of the curve of σ_{12} versus $\dot{\gamma}$ will depend on the degree of entanglement N. For asymptotically large N, the fluctuation effects are killed off by the exponential dependence of τ_ξ on N in eq 19, and the theory without fluctuations is recovered. Thus, the slope of the $\sigma_{12}(\dot{\gamma})$ curve is predicted to become flatter as the entanglement density increases, a prediction in accord with experimental observations. In addition, the reduction in zero-shear viscosity η_0 produced by fluctuations (Figure 15b) will also disappear at large N. This implies that at smaller N the dependence of η_0 on N will be somewhat greater than the N^3 power law obtained from reptation alone. A steeper N dependence of η_0 is in accord with experiments, which show the famous $N^{3.4}$ power law. For $N = 17$, the fluctuations reduce the longest relaxation time to a value τ_1 that is about 5 times shorter than the reptation time τ_d. Thus, the ratio of the longest relaxation time to the Rouse time is reduced to $\tau_1/\tau_s = 0.2\tau_d/\tau_s = 0.2 \times 3N = 10$, for the case $N = 17$. This value, $\tau_1/\tau_s = 10$, corresponds roughly to the value of τ_1/τ_s inferred for the polystyrene solution described in Figures 1 and 2. Figure 16 shows that the CCR theory, with fluctuations, makes possible essentially quantitative predictions of the shapes of the curves of shear stress and first normal stress difference. There is no room here for further direct comparisons of experiment and theory, which will therefore be deferred to a future publication.

The predictions of the nonlinear modulus after a step-shear strain are shown in Figure 17a. These calculations omit fluctuation effects, which are not especially important in this deformation history. Note that, as expected, the moduli for different strains nearly coincide at short times, unlike the predictions of the simple model in Figure 13a, which used the IAA. Figure 17b

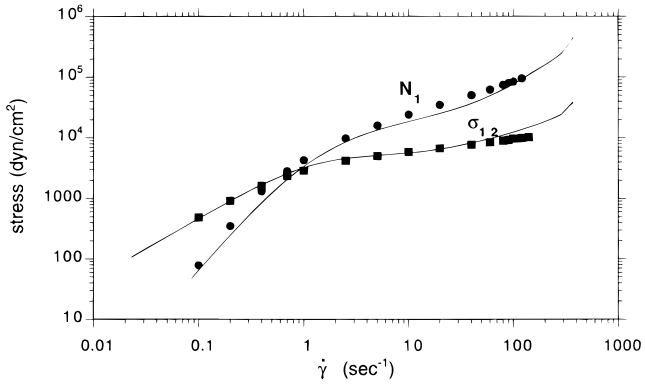

Figure 16. Measurements (symbols) versus predictions (lines) of the shear stress and first normal stress difference for a 10% by weight solution of polystyrene of molecular weight 2 million in tricresyl phosphate at 40 °C using the Rheometrics ARES rheometer. For the theory, $3N = 50$, which is approximately the experimental value, and $\tau_d = 2.08$ s and $G_N^0 = 11\,500$ dyn/cm^2 were obtained by a best fit to the data. This data set resolves the low-shear rate behavior better than does the data set in Figure 1 and so allows more accurate determination of τ_d.

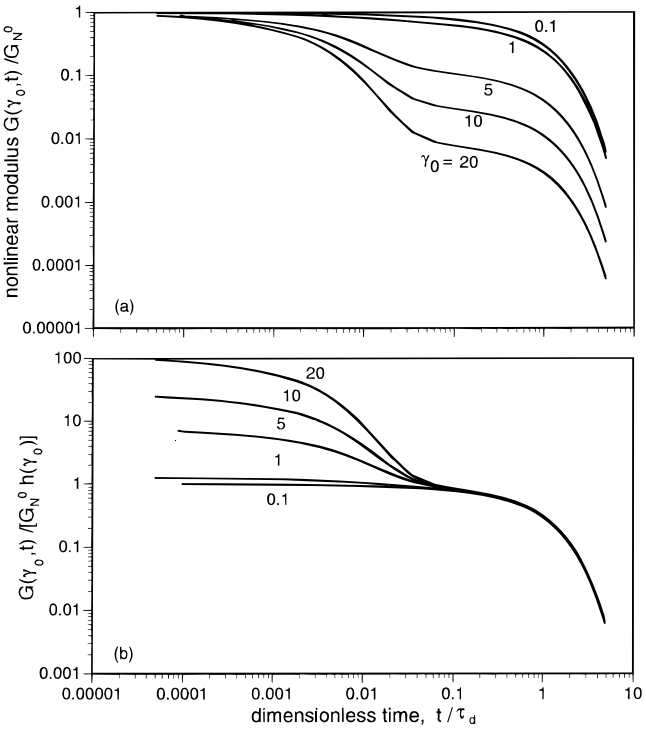

Figure 17. (a) Nonlinear modulus $G(\gamma_0,t)/G_N^0$ after step strains γ_0 of magnitudes shown, predicted by the contour-variable model with no fluctuation effects (eqs 14−18). (b) The results in part a are divided by the DE damping function $h(\gamma_0)$ without the independent alignment approximation.

shows that when the nonlinear modulus is divided by the DE damping function $h(\gamma_0)$ (derived without the IAA), the predictions all nearly collapse onto a single line at long times, $t/\tau_s \gg 1$, in agreement with experiments.

As attractive as these features of the theory are, from the standpoint of validation of the theory, they are less important than the predictions for the transients in χ (see Figure 2), which, as will be recalled from section II, are *not* predicted to be nonmonotonic by the CCR mechanism, when incorporated into the simplified model. It turns out that these transients are also absent

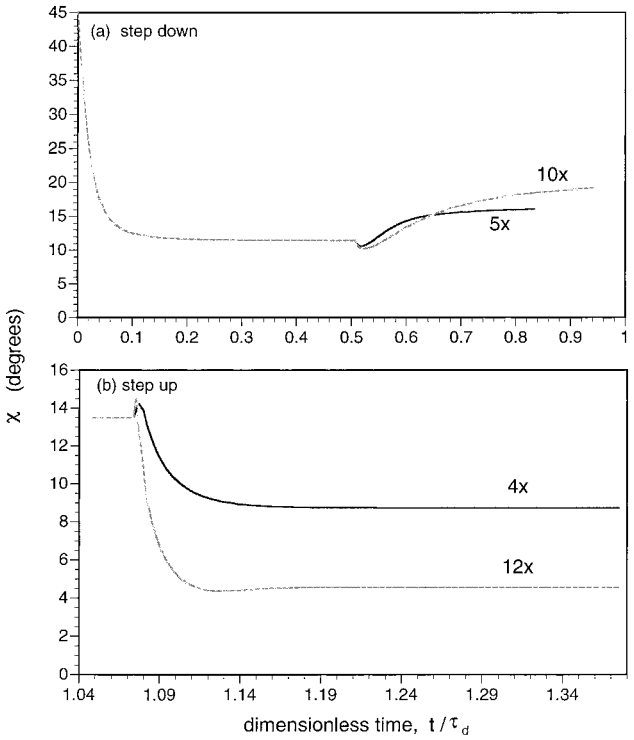

Figure 18. Time-dependent extinction angle χ as a function of time after startup of steady shearing flow and attainment of steady state followed by (a) a stepdown in dimensionless shear rate $\dot{\gamma}\tau_s$ from 2 to 0.4 and from 2 to 0.2 and (b) a stepup in dimensionless shear rate $\dot{\gamma}\tau_s$ from $\dot{\gamma}\tau_s = 1$ to 4 and from 1 to 12, as predicted by the contour-variable model with fluctuations (eqs 15−20).

from the predictions of eqs 13−18 but appear when the fluctuation effects are included, using eqs 19 and 20. Figure 18 shows the χ transients predicted in (a) startup followed by a stepdown in shear rate and (b) steady state followed by a stepup in rate. The predicted results are remarkably similar to the experimental transients reported in Figure 2a,b!

The mechanism of these transients is revealed by considering the tube stretch $\lambda(s)$ and orientation $\chi(s)$ as functions of the tube coordinate s after a stepup or stepdown in shear rate. While a detailed discussion is beyond the scope of this preliminary paper, we give a brief summary of our findings here. Examination of $\lambda(s)$ and $\chi(s)$ shows that the fluctuations greatly decrease the orientation at the ends of the chain. In addition, at high shear rate, $\dot{\gamma}\tau_s > 1$, the tube segments are significantly stretched ($\lambda > 1$) to an extent that depends on shear rate and on the locations along the tube contour. When the shear rate is suddenly stepped down, the tube stretching is suddenly reduced. As a result, chain ends, which are in highly disoriented tube segments before the stepdown, are drawn into inner tube segments that are less influenced by fluctuation effects and hence more aligned. This produces a rapid increase in average orientation. Eventually, however, fluctuations and reptation will relax the tube segments newly occupied by the chain ends, and the average degree of orientation of the chain will decrease again. Thus, after a stepdown in $\dot{\gamma}$, χ will at first *decrease* (corresponding to *increased* average orientation of tube segments) and then will increase to a value higher than the starting value, since the final shear rate is lower than the initial one.

In the case of a stepup in shear rate, the tube stretch is immediately increased but is increased nonuniformly along the tube. The chain segments near the ends of the molecule experience a greater drag force and so the tube is stretched more there. However, the segments near the end have the least orientation. Therefore, the contribution to the stress and orientation from these relatively disoriented segments is enhanced at first. Hence, χ initially increases. However, these stretched segments are quickly oriented by the flow and retract, reducing their stress contributions and leading to a rapid decrease in χ, as observed. The good correspondence of these detailed time-dependent predictions with experimental results provides significant support for the model developed here. The results also strongly support the validity of the tube concept, even in fast flows where convection continually dissolves and reconstitutes the tube.

Thus, all of the phenomena described in the Introduction are captured almost quantitatively by the contour-variable theory described in section III.B, with one exception. While the χ undershoot observed on startup of shearing flow from a state of rest (Figure 2a) is indeed predicted by the contour-variable theory, it is predicted to be so small an effect that it does not show up in Figure 18a. Exploration of possible reasons for this shortcoming of the theory will be left to future work.

IV. Summary

We have extended the DEMG theory for the nonlinear rheological properties of entangled, flexible polymers by including a mechanism of CCR, inspired by ideas of Marrucci and Ianniruberto. With this mechanism, constraints that define a tube disappear (and are renewed) at a rate proportional to the rate of retraction of the chains defining the tube. When a constraint is thereby released, the orientation of the corresponding tube segment is randomized if the chain within it is slack, but if the chain is taut, the tube segment disappears, thereby shortening the tube. With these mechanisms of constraint release, the resulting theory captures many of the prominent nonlinear rheological properties of entangled flexible polymers under fast flows, i.e., at shear rates $\dot{\gamma}$ greater than the inverse reptation time $1/\tau_d$. These are shear rates for which the DE and DEMG theories fail.

The rheological phenomena captured by the new theory include a nearly constant shear stress as a function of shear rate $\dot{\gamma}$ for $\dot{\gamma}$ greater than the inverse reptation time and a first normal stress difference that increases with a power of unity or less in this shear-rate range. These steady-state phenomena had already been described by a simple theory of Marrucci and Ianniruberto. Our more complete theory also predicts transient phenomena, including an initial rate of stress relaxation after cessation of steady shear that increases with shear rate, and nonmonotonic transients in extinction angle χ on stepup or stepdown in the shear rate. Successful features of the DEMG theory, such as the response to a step-shear strain and overshoots in shear stress and first normal stress difference on shear startup, are retained in the new theory.

The general theory can be written in a simplified form in which it is assumed that all parts of the molecule share the same orientation and degree of stretch or in a contour-variable form in which orientation and stretch are functions of the tube coordinate. Both versions of

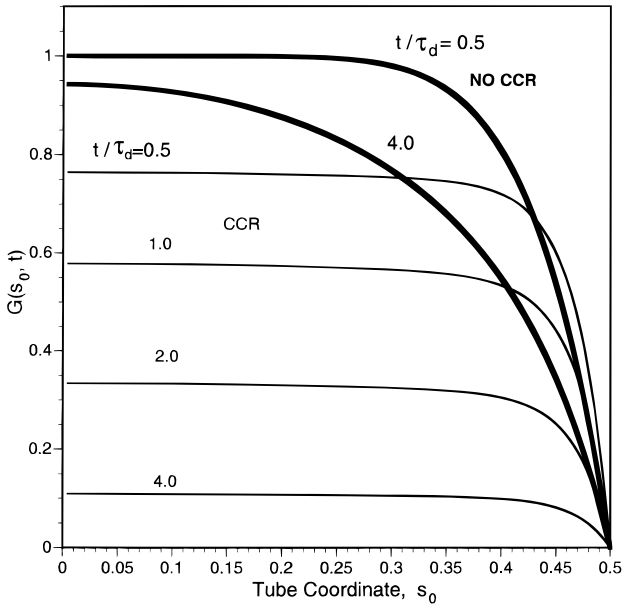

Figure 19. Tube survival probability $G(s,t)$ versus tube coordinate s for tube segments created at time 0 in a steady-state shearing flow with $\dot{\gamma}\tau_d = 50$ and $\tau_d/\tau_s = 50$. The thick lines are predictions of the DEMG theory with no CCR; the thin lines are the predictions of eq 14 with CCR.

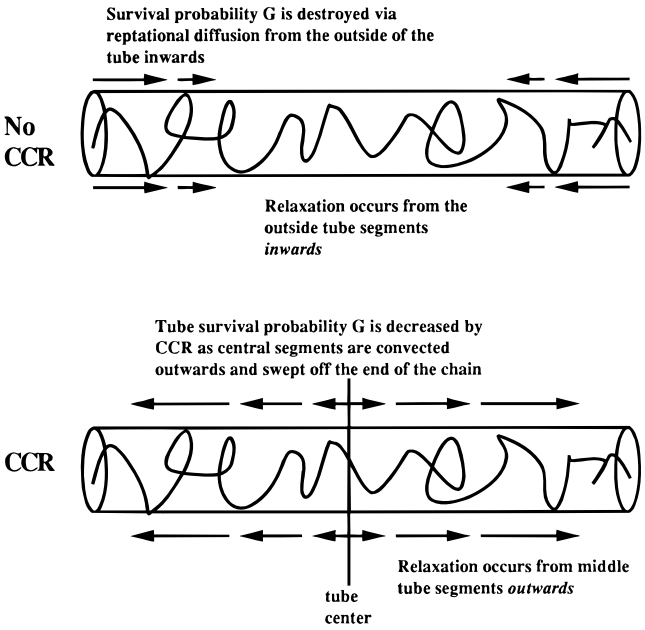

Figure 20. Illustration of the process of relaxation when (top) no CCR is present, so that reptation is the only mechanism of relaxation, and (bottom) when CCR is the dominant mechanism of relaxation.

the theory yield qualitatively similar predictions, except that the χ transients are only captured in the contour-variable theory and only then when primitive-path-length fluctuations are included. A subsequent paper will describe how both the simplified and the contour-variable versions of the theory can be extended to account for polydispersity.

Acknowledgment. We are grateful for advice from Pino Marrucci and Giovanni Ianniruberto, especially for helping us understand the importance of tube stretching in the rate of relaxation after steady shear. We also acknowledge valuable discussions with Hiroshi Watanabe and with Ali Berker. We are also grateful to Cataleeya Pattamaprom for providing steady-state data on polystyrene solutions. This work was supported by The Japanese Society for the Promotion of Science (JSPS).

Appendix A: Constraint-Release Mechanism of Relaxation and Boundary-Layer Analysis

In this appendix, we describe the process of stress relaxation during fast, steady flows ($\dot{\gamma} \gg 1/\tau_d$) of entangled polymers and explain why the simplified model of section II captures the basic phenomena nearly as well as the more complete contour-variable model of section III.

In Figure 19, we plot the steady-state tube survival probability function $G(s_0,t)$ of the contour-variable model as a function of the tube coordinate s_0 at various times t after creation of the tube segment at time $t' = 0$. (We assume that the flow began at some time in the remote past; i.e., at $-\infty$.) $G(s_0,t)$ is calculated from eq 14 for a melt with $N = 16.7$ entanglements ($\tau_d = 50\tau_s$) and a steady shear rate of $\dot{\gamma} = 50/\tau_d$, both with and without the constraint-release term. Thus, in this example calculation, the flow is fast compared to the orientational relaxation rate but not fast enough to generate significant lengthening of the tube. Hence, while the results are plotted against the unstretched tube coordinate s_0, nearly identical results would be obtained by plotting against the stretched tube coordinate s.

The thick lines in Figure A1 show $G(s_0,t)$ with no CCR, while for the thin lines CCR is turned on. In the absence of CCR, reptation of the chain out of the tube is the only mechanism by which occupied tube segments are lost. Hence, diffusion occurs from the chain ends *inward*, as is evident from the boundary-layer structure of the function $G(s_0,t)$, where G remains near unity, except near the chain ends. Even as the time t increases, diffusion is unable to reduce significantly the value of G in the center of the tube, because the tube segments most affected by diffusion are convected off the end of the chain, while the few segments that started near the tube center are stretched in length so that they comprise almost the entire contour length from $-L/2$ to $L_0/2$. As these segments are stretched, they carry their high survival probability with them, which remains near unity. Thus, like a guppy trying to swim randomly against the jet from a fire hose, diffusive penetration of the boundary layers toward the tube center is overwhelmed by the rapid convection and stretching of central tube segments, which presses the boundary layers back toward the chain ends; see Figure 20 (top).

When CCR is present, the situation is entirely different, however, as shown by the thin lines in Figure 19. Tube segments are lost not just at the chain ends but along the entire length of the tube. Hence, there is a dominant central region where G is independent of s_0, and the height of this central region is eroded with time t. Thus, with CCR, reptative diffusion from the chain ends is almost irrelevant. Instead, orientational relaxation occurs by the combination of CCR and probability convection along the tube. At large t, tube segments created anywhere except near the center of the tube have been swept off the end of the tube. The surviving tube segments are therefore those few segments that began near the center of the tube at time 0 and so still reside on the tube at time t. These segments

have been stretched to nearly the entire length of the occupied tube and have been acted on by CCR for a relatively long time, long enough to greatly reduce their survival probability at large t. Thus, with CCR present, loss of tube survival probability occurs by constraint release on central tube segments as they are *convected outward*. This contrasts with the *inward diffusive* mechanism of relaxation in the absence of CCR; see Figure 20.

The near uniformity of the tube survival probability $G(s_0,t)$ explains the accuracy of the simplified model, which neglects dependences on the chain contour variable. We can make this explanation more precise by doing a boundary-layer analysis on eq 14. In dimensionless form, this equation is

$$\frac{\partial G}{\partial t^*} = \frac{1}{\pi^2 \dot\gamma \tau_d}\frac{\partial^2 G}{\partial s^{*2}} - \langle v^*\rangle \frac{\partial G}{\partial s^*} + f\left(\frac{\partial s^*}{\partial s_0^*}\right)\left[\frac{2L_0}{L(t)}\left(\frac{\partial s^*}{\partial t^*} - \langle v^*\rangle\right)_{s^*=1/2}\right]G \quad \text{(A1)}$$

where the dimensionless quantities are defined as

$$t^* \equiv t\dot\gamma; \quad s^* \equiv \frac{s}{L_0}; \quad \langle v^*\rangle \equiv \frac{\langle v\rangle}{\dot\gamma L_0} \quad \text{(A2)}$$

Note that the time has been multiplied by the shear rate in accord with Marrucci and Ianniruberto's arguments for fast flows.[2,5] The solution to this equation is controlled by the magnitude of the dimensionless quantity $\dot\gamma\tau_d$. If we restrict consideration to flows that are fast enough that CCR is important yet slow enough that chain stretching is unimportant, $\partial s^*/\partial s_0^* = 1$, and the analysis is greatly simplified. Thus, at steady state with no stretch, eq A1 simplifies to

$$\frac{\partial G}{\partial t^*} = \frac{1}{\pi^2 \dot\gamma \tau_d}\frac{\partial^2 G}{\partial s^{*2}} - \langle v^*\rangle \frac{\partial G}{\partial s^*} - 2\langle v^*\rangle|_{s^*=1/2} G \quad \text{(A3)}$$

The boundary conditions are

$$G = 0; \quad \text{at } s^* = -{}^1/_2,\ {}^1/_2$$

At long times (to be defined shortly), eq A3 can be solved by separation of variables:

$$G(s^*,t^*) = S(s^*)\ T(t^*) \quad \text{(A4)}$$

This separation of variables implies that although the height of the curve $G(s^*,t^*)$ decreases with time, its shape remains constant. Substituting eq A4 into eq A3 gives

$$\frac{1}{T}\frac{dT}{dt^*} + 2\langle v^*\rangle|_{s^*=1/2} = \frac{1}{\pi^2\dot\gamma\tau_d}\frac{1}{S}\frac{d^2S}{ds^{*2}} - \langle v^*\rangle\frac{1}{S}\frac{dS}{ds^*} = \text{constant} \quad \text{(A5)}$$

The value of the constant can be determined by noting that on the centerline of the tube the velocity is identically zero. Since $\dot\gamma\tau_d$ is large, both terms on the right side of eq A5 are very small on the centerline and hence nearly zero everywhere. This allows us to solve for the function $T(t^*)$:

$$T(t^*) = \exp\{-2\langle v^*\rangle|_{s^*=1/2} t^*\} \quad \text{(A6)}$$

Thus, the tube survival probability decreases exponentially because of CCR.

The equation for $S(s^*)$ becomes

$$\frac{1}{\pi^2\dot\gamma\tau_d}\frac{d^2S}{ds^{*2}} - \langle v^*\rangle\frac{dS}{ds^*} = 0 \quad \text{(A7)}$$

For steady-state shearing flow, the relative tube velocity is approximately a linear function of s^*:

$$\langle v^*\rangle \approx S_{12} s^* \quad \text{(A8)}$$

Given the large magnitude of $\dot\gamma\tau_d$, eq A7 has the structure of a singular perturbation problem and can be solved using a matched asymptotic expansion. The approximate dimensionless thickness of the boundary layer δ^* can be determined by balancing the two terms within the boundary layer, giving

$$S(s^*) = 1 - \exp[-(1/2 - s^*)/\delta] \quad \text{(A9)}$$

with

$$\delta^* \approx \frac{1}{\pi^2\dot\gamma\tau_d\langle v^*\rangle} \approx \frac{2}{\pi^2\dot\gamma\tau_d S_{12}} \quad \text{(A10)}$$

Combining eqs A9 and A10 with eqs A4 and A6 and restoring dimensional quantities give the complete solution:

$$G(s,t) = \exp[-S_{12}\dot\gamma t][1 - \exp\{-{}^1/_2\pi^2\dot\gamma\tau_d S_{12}({}^1/_2 - s/L)\}] \quad \text{(A11)}$$

This boundary-layer solution is valid once the boundary layer has been established by diffusion in from the end of the tube. The dimensionless time t_{diff}/τ_d for this to occur is roughly

$$t_{diff}/\tau_d \approx \frac{\delta^2}{D} = \frac{4}{\pi^2\dot\gamma^2\tau_d {S_{12}}^2} \quad \text{(A12)}$$

For the case treated in Figure 19, $\dot\gamma\tau_d = 50$ and using the result from appendix B that $S_{12} \approx 0.12$ in the intermediate shear rate regime, we find that the boundary-layer structure is established very rapidly, in a dimensionless time of only $t_{diff}/\tau_d \approx 0.004$. The dimensionless depth δ/L_0 of the boundary layer, from eq A11, is around 0.03, which agrees with the exact results shown in Figure 1. At moderate or large t/τ_d, the boundary layer is therefore much shallower than that for pure reptation; compare the thin and thick lines in Figure 19 for $t/\tau_d = 4$. The shallowness of the boundary layer when CCR is present means that the survival probability $G(s,t,t')$ is nearly uniform across almost the entire tube. Hence, the dependence of G on s can be neglected to a good approximation in fast flows. Neglect of the dependence on s leads to the simplified model described in section II. The shallowness of the boundary layer explains why the simplified model gives almost the same predictions as the "contour-variable" model, at least when contour-length fluctuations are neglected.

Appendix B: Steady-State Behavior

1. Shear. Some analytical and semianalytical results can be derived from the simple CCR constitutive equation (10)−(13) in steady-state shearing flows. First, we

rewrite eqs 10 and 11 by defining a relaxation time τ as

$$\frac{1}{\tau} = \frac{1}{\lambda^2\tau_d} + f(\lambda)\left(\kappa{:}\mathbf{S} - \frac{\dot{\lambda}}{\lambda}\right) \tag{B1}$$

Equation 11 can then be written as

$$\mathbf{S} = \int_{-\infty}^{t} \frac{dt'}{\tau(t')} \exp\left[-\int_{t'}^{t} \frac{dt''}{\tau(t'')}\right] \mathbf{Q}(\mathbf{E}(t,t')) \tag{B2}$$

Defining $\alpha \equiv \dot{\gamma}\tau$, and assuming steady state, eq B1, when divided by $\dot{\gamma}$, becomes

$$\frac{1}{\alpha} = \frac{1}{\lambda^2\tau_d\dot{\gamma}} + f(\lambda)\, S_{12} \tag{B3}$$

where S_{12} is given by eq 11. Defining $x \equiv \dot{\gamma}(t - t')$, this becomes

$$S_{12} \equiv \frac{1}{\alpha}\int_0^\infty dx\, \exp(-x/\alpha) Q_{12}(x) \equiv I(\alpha) \tag{B4}$$

Finally, eq 12 reduces to

$$\frac{1}{2}(\lambda + 1)\dot{\gamma}\tau_s S_{12} = \lambda - 1 \tag{B5}$$

To obtain the asymptotic behavior of the function $I(\alpha)$, notice that

$$Q_{12}(x) = \frac{x}{5} \quad (\text{for } x \ll 1) \tag{B6}$$

$$Q_{12}(x) = \frac{1}{x} \quad (\text{for } x \gg 1) \tag{B7}$$

Therefore, for $\alpha \ll 1$,

$$I(\alpha) = \frac{1}{\alpha}\int_0^\infty dx\, \exp(-x/\alpha)\frac{x}{5} = \frac{\alpha}{5} \tag{B8}$$

and for $\alpha \gg 1$,

$$I(\alpha) = \frac{\ln \alpha}{\alpha} \tag{B9}$$

This last result can be shown as follows. First break the integral in eq B4 into two pieces:

$$I(\alpha) = \frac{1}{\alpha}\left[\int_0^\infty dx\, \exp(-x/\alpha)\left(Q_{12}(x) - \frac{1}{x+1}\right) + \int_\infty^0 dx\, \exp(-x/\alpha)\frac{1}{x+1}\right] \tag{B10}$$

The first integral in eq B10 approaches a constant when $\alpha \to \infty$. Defining $y \equiv x/\alpha$, the second integral can be integrated by parts:

$$\int_0^\infty dx\, \exp(-x/\alpha)\frac{1}{x+1} = \int_0^\infty dy\, \exp(-y)\frac{1}{y + 1/\alpha} \tag{B11}$$

$$= \left[\ln\left(y + \frac{1}{\alpha}\right)e^{-y}\right]_0^\infty + \int_0^\infty dy \times \exp(-y)\ln(y + 1/\alpha) \tag{B12}$$

$$= \ln \alpha + \text{const} \tag{B13}$$

Now we consider the limit of $3N = \tau_d/\tau_s \gg 1$. In this case, there is an intermediate region of shear rate $\dot{\gamma}$ for which $1/\tau_d \ll \dot{\gamma} < 1/\tau_s$. In this limit we can set $\dot{\gamma}\tau_d = \infty$ with $\dot{\gamma}\tau_s = 0$ in eqs B3−B5. This gives

$$\lambda = 1 \tag{B14}$$

and

$$S_{12} = I(\alpha^*) \tag{B15}$$

where α^* is the solution to

$$\alpha^* I(\alpha^*) = 1 \tag{B16}$$

A numerical solution of this equation gives

$$\alpha^* = 8.1; \quad S_{12} = 0.123 \tag{B17}$$

The value of $S_{11} - S_{22}$ can be obtained by replacing Q_{12} in eq B4 with $Q_{11} - Q_{22}$ and integrating, using $\alpha = \alpha^*$. Since $\boldsymbol{\sigma} = 5G_N^0\mathbf{S}$, this gives for the intermediate shear-rate region

$$S_{12} = 0.123; \quad S_{11} - S_{22} = 0.669$$

$$\sigma_{12}/G_N^0 = 0.615; \quad N_1/\sigma_{12} = 5.44$$

$$\chi = 0.5 \tan^{-1}[2S_{12}/(S_{11} - S_{22})] = 10.1° \tag{B18}$$

In the high-shear-rate regime, where $\dot{\gamma}\tau_s \gtrsim 1$, eq B3 becomes

$$\frac{1}{\alpha} = f(\lambda)\, S_{12} \tag{B19}$$

Using eq B9 and $S_{12} = I(\alpha)$, we find that

$$\lambda = 1 + \ln(\ln(\alpha)), \quad \text{for } f(\lambda) = e^{-(\lambda-1)}$$

$$\lambda = \ln(\alpha), \quad \text{for } f(\lambda) = 1/\lambda \tag{B20}$$

Substituting this into eq B5, we have

$$\frac{\dot{\gamma}\tau_s}{\alpha} = \frac{\ln(\ln \alpha)}{\ln \alpha[(1 + 0.5\ln(\ln \alpha)]}, \quad \text{for } f(\lambda) = e^{-(\lambda-1)}$$

$$\frac{\dot{\gamma}\tau_s}{\alpha} = \frac{2(\ln(\alpha) - 1)}{\ln \alpha(\ln(\alpha) + 1)}, \quad \text{for } f(\lambda) = \frac{1}{\lambda} \tag{B21}$$

We now write

$$\alpha = c(\dot{\gamma})\, \dot{\gamma}\tau_s \tag{B22}$$

where $c(\dot{\gamma})$ is the inverse of the right side of eq B21:

$$c(\dot{\gamma}) = \frac{\ln \alpha[(1 + 0.5\ln(\ln \alpha)]}{\ln(\ln(\alpha))}, \quad \text{for } f(\lambda) = e^{-(\lambda-1)}$$

$$c(\dot{\gamma}) = \frac{\ln \alpha(\ln(\alpha) + 1)}{2(\ln(\alpha) - 1)}, \quad \text{for } f(\lambda) = \frac{1}{\lambda} \tag{B23}$$

We note that $c(\dot{\gamma})$ depends very weakly on $\dot{\gamma}$. If we take it to be almost a constant, using eqs B19, B20, and B22, we obtain

$$S_{12} = \frac{\ln(c\dot{\gamma}\tau_s)}{c\dot{\gamma}\tau_s} \tag{B24}$$

$S_{11} - S_{22}$ is nearly unity. We can evaluate the near-constant c by setting $\alpha = \alpha^* = 8.1$ in eq B23. This gives $c \approx 3.88$ for $f(\lambda) = \exp(-(\lambda - 1))$, and $c \approx 2.96$ for $f(\lambda) =$

$1/\lambda$. We can obtain χ in this high-shear-rate regime from the ratio $S_{12}/(S_{11} - S_{22})$, as usual. The stress tensor $\boldsymbol{\sigma}$ is $5G_N^0$ times the **S** tensor.

Summarizing, for the high-shear-rate region, we obtain

$$\lambda = 1 + \ln(\ln(c\dot{\gamma}\tau_s)), \quad \text{for } f(\lambda) = e^{-(\lambda-1)}$$

$$\lambda = \ln(c\dot{\gamma}\tau_s), \quad \text{for } f(\lambda) = 1/\lambda \tag{B25}$$

$$\chi \approx \frac{\ln(c\dot{\gamma}\tau_s)}{c\dot{\gamma}\tau_s} \tag{B26}$$

$$\frac{\sigma_{12}}{G_N^0} = 5\lambda^2\frac{\ln(c\dot{\gamma}\tau_s)}{c\dot{\gamma}\tau_s}; \quad \frac{N_1}{G_N^0} = 5\lambda^2 \tag{B27}$$

where we can take $c \approx 3.88$ for $f(\lambda) = \exp(-(\lambda - 1))$ and $c \approx 2.96$ for $f(\lambda) = 1/\lambda$. For $\dot{\gamma}\tau_s = 100$, these formulas give $\lambda = 2.79$, $\chi = 0.9°$, $\sigma_{12}/G_N^0 = 0.60$, and $N_1/G_N^0 = 39$ for $f(\lambda) = \exp(-(\lambda - 1))$ and $\lambda = 5.69$, $\chi = 1.1°$, $\sigma_{12}/G_N^0 = 3.11$, and $N_1/G_N^0 = 162$ for $f(\lambda) = 1/\lambda$. These values are in reasonable agreement with the results plotted in Figures 7 and 8.

2. Uniaxial Extension. For uniaxial extension with "1" stretch direction, eq B3 is modified to

$$\frac{1}{\alpha} = \frac{1}{\lambda^2\tau_d\dot{\gamma}} + e^{-(\lambda-1)}(S_{11} - S_{22}) \tag{B28}$$

where $\alpha \equiv \dot{\epsilon}\tau$, with $\dot{\epsilon}$ the rate of uniaxial strain. $S_{11} - S_{22}$ is given by

$$S_{11} - S_{22} \equiv \frac{1}{\alpha}\int_0^\infty dx\, \exp(-x/\alpha)[Q_{11}(x) - Q_{22}(x)] \equiv I(\alpha) \tag{B29}$$

The counterpart to eq B5 is

$$\frac{1}{2}(\lambda + 1)\dot{\epsilon}\tau_s(S_{11} - S_{22}) = \lambda - 1 \tag{B30}$$

For intermediate strain rates, $1/\tau_d \ll \dot{\epsilon} \ll 1/\tau_s$, $\lambda = 1$, and $S_{11} - S_{22} = I(\alpha^*)$, where α^* is the solution to $\alpha^* I(\alpha^*) = 1$. A numerical solution gives $\alpha^* = 1.65$ and $S_{11} - S_{22} = 0.607$. Hence, the dimensionless extensional stress is $(\sigma_{11} - \sigma_{22})/G_N^0 = 5(S_{11} - S_{22}) = 3.04$.

At high extension rates, $S_{11} - S_{22} \to 1$. The solution to eq B30 is then

$$\lambda = \frac{1 + \dot{\epsilon}\tau_s/2}{1 - \dot{\epsilon}\tau_s/2}$$

This produces "run-away" chain stretching at an extension rate $\dot{\epsilon} = 2/\tau_s$.

Appendix C: Step-Shear Behavior

After a step shear, eqs B1 and 12 reduce to

$$\frac{1}{\tau} = \frac{1}{\lambda^2\tau_d} - \frac{\dot{\lambda}}{\lambda}f(\lambda) \tag{C1}$$

$$\dot{\lambda} = -\frac{\lambda - 1}{\tau_s} + \frac{\dot{\lambda}}{2\lambda}(\lambda - 1) \tag{C2}$$

The solution of eq C2 with the initial condition $\lambda(0) = \lambda_0$, which is the stretch immediately after the step, is

$$\frac{\lambda - 1}{\lambda_0 - 1}\sqrt{\frac{\lambda_0}{\lambda}} = \exp(-t/\tau_s) \tag{C3}$$

The asymptotic behavior of this equation is

$$\lambda(t) = \lambda_0\left(1 - \frac{2(\lambda_0 - 1)}{\lambda_0 + 1}\frac{t}{\tau_s}\right); \quad \text{for } t \ll \tau_s \tag{C4}$$

$$\lambda(t) = 1 + \frac{\lambda_0 - 1}{\sqrt{\lambda_0}}\exp(-t/\tau_s); \quad \text{for } t \gg \tau_s \tag{C5}$$

Thus, for $t \gg \tau_s$, $\lambda(t)$ quickly approaches unity.

At time t after the step shear strain γ_0, eq B2 for the tensor **S** reduces to

$$\mathbf{S} = \exp\left(-\int_0^t \frac{dt'}{\tau(t')}\right)\mathbf{Q}(\gamma_0) \tag{C6}$$

Using eq C1, this can be rewritten as

$$\mathbf{S} = \exp(-g(t,\gamma_0))\mathbf{Q}(\gamma_0) \tag{C7}$$

where

$$g(t,\gamma_0) = \int_0^t \frac{dt'}{\tau(t')} = g_1(t,\gamma_0) + g_2(t,\gamma_0) \tag{C8}$$

with

$$g_1(t,\gamma_0) = \int_0^t \frac{dt'}{\tau_d\lambda^2(t')} \tag{C9}$$

and

$$g_2(t,\gamma_0) = -\int_0^t dt' \frac{\dot{\lambda}(t')}{\lambda(t')}f(\lambda(t')) \tag{C10}$$

Since $\lambda(t)$ approaches unity for $t \gg \tau_s$, $g_1(t,\gamma_0)$ has the following asymptotic form:

$$g_1(t,\gamma_0) = \frac{1}{\tau_d}(t - C_1(\gamma_0)\,\tau_s)) \tag{C11}$$

where

$$C_1(\gamma_0) = \frac{1}{\tau_s}\int_0^\infty dt\left(1 - \frac{1}{\lambda^2}\right) = \frac{1}{\tau_s}\int_{\lambda_0}^1\left(1 - \frac{1}{\lambda^2}\right)\frac{d\lambda}{\dot{\lambda}} = \int_1^{\lambda_0}\frac{(\lambda + 1)^2}{2\lambda^3}\,d\lambda$$

$$= \frac{1}{2}\left[\ln(\lambda_0) - 2\left(\frac{1}{\lambda_0} - 1\right) - \frac{1}{2}\left(\frac{1}{\lambda_0^2} - 1\right)\right] \tag{C12}$$

On the other hand, by using eq C2, eq C10 can be written as

$$g_2(t,\gamma_0) = \int_{\lambda(t)}^{\lambda_0} d\lambda\,\frac{f(\lambda)}{\lambda} \tag{C13}$$

For $t \gg \tau_s$, $\lambda(t) \approx 1$. Therefore, $g_2(t,\gamma_0)$ may be approximated as

$$g_2(t,\gamma_0) = C_2(\gamma_0) = \int_1^{\lambda_0} d\lambda \frac{f(\lambda)}{\lambda} \tag{C14}$$

$C_2(\gamma_0)$ is an increasing function of γ_0. It starts with 0 when $\gamma_0 \rightarrow 0$ and approaches the asymptotic value

$$\begin{aligned} C_2(\infty) &= \int_1^{\infty} d\lambda \frac{f(\lambda)}{\lambda} \\ &= 0.5963, \quad \text{for } f(\lambda) = \exp(-(\lambda - 1)) \\ &= 1, \quad \text{for } f(\lambda) = 1/\lambda \end{aligned} \tag{C15}$$

In summary, the stress for $t \gg \tau_s$ is written as

$$\sigma_{12}(t,\gamma_0) = G_N^0 \gamma_0 h_{DE}(\gamma_0)\, h_{CR}(\gamma_0) \exp(-t/\tau_d) \tag{C16}$$

where

$$h_{CR}(\gamma_0) = \exp\left(\frac{C_1(\gamma_0)\,\tau_s}{\tau_d} - C_2(\gamma_0)\right) \tag{C17}$$

with

$$C_1(\gamma_0) = \frac{1}{2}\left[\ln(\lambda_0) - 2\left(\frac{1}{\lambda_0} - 1\right) - \frac{1}{2}\left(\frac{1}{\lambda_0^2} - 1\right)\right] \tag{C18}$$

and

$$C_2(\gamma_0) = \int_1^{\lambda_0(\gamma_0)} d\lambda \frac{f(\lambda)}{\lambda} \tag{C19}$$

and $h_{DE}(\gamma_0)$ is the original DE damping function; i.e., $h_{DE}(\gamma_0) \equiv Q_{12}(\gamma_0)/\gamma_0$.

Finally, $\lambda_0(\gamma_0)$ is obtained from the solution of eq 12 with $\dot{\gamma}\tau_s \rightarrow \infty$. This gives

$$\lambda_0(\gamma_0) = \exp\left(\int_0^{\gamma_0} d\gamma\, Q_{12}(\gamma)\right) \tag{C20}$$

References and Notes

(1) Marrucci, G.; Grizzuti, N. *Gazz. Chim. Ital.* **1988**, *118*, 179.
(2) Marrucci, G. *J. Non-Newtonian Fluid Mech.* **1996**, *62*, 279.
(3) Ianniruberto, G.; Marrucci, G. *J. Non-Newtonian Fluid Mech.* **1996**, *65*, 241.
(4) Bercea, M.; Peiti, C.; Dimionescu, B.; Navard, P. *Macromolecules* **1993**, *26*, 7095.
(5) Marrucci, G.; Ianniruberto, G. *Macromol. Symp.* **1997**, *117*, 233.
(6) Pearson, D. S. *Rubber Chem Technol., Rubber Rev.* **1987**.
(7) Viovy, J. L.; Rubinstein, M.; Colby, R. H. *Macromolecules* **1991**, *24*, 3587.
(8) Tsenoglou, C. *Polym. Prepr.* (*Am. Chem. Soc., Div. Polym. Chem.*) **1987**, *28*, 185.
(9) des Cloizeaux, J. *J. Europhys. Lett.* **1988**, *5*, 437; **1988**, *6*, 475.
(10) Wasserman, S. H.; Graessley, W. W. *J. Rheol.* **1992**, *36*, 543.
(11) Tuminello, W. H. *Polym. Eng. Sci.* **1986**, *26*, 1339.
(12) Mead, D. W. *J. Rheol.* **1994**, *38*, 1797.
(13) Mead, D. W. *J. Rheol.* **1996**, *40*, 2877.
(14) Milner, S. T. *J. Rheol.* **1996**, *40*, 303.
(15) Ball, R. C.; McLeish, T. C. B. *Macromolecules* **1989**, *22*, 1911.
(16) Doi, M.; Edwards, S. F. *J. Chem. Soc., Faraday Trans. 2* **1978**, *74*, 1789, 1802, 1818.
(17) Doi, M.; Edwards, S. F. *J. Chem. Soc., Faraday Trans. 2* **1979**, *75*, 32.
(18) Doi, M.; Edwards, S. F. *The Theory of Polymer Dynamics*; Oxford Press: New York, 1986.
(19) Pearson, D. S.; Herbolzheimer, E.; Grizzuti, N.; Marrucci, G. *J. Polym. Sci., Part B: Polym. Phys. Ed.* **1991**, *29*, 1589.
(20) Mead, D. W.; Leal, L. G. *Rheol. Acta* **1995**, *34*, 339.
(21) Mead, D. W.; Yavich, D.; Leal, L. G. *Rheol. Acta* **1995**, *34*, 360.
(22) Stratton, R. A. *J. Colloid Interface Sci.* **1966**, *22*, 517.
(23) Ferry, J. D. *Viscoelastic Properties of Polymers*, 3rd ed.; John Wiley & Sons: New York, 1980.
(24) Gleissle, W. *Rheol. Acta* **1982**, *21*, 484.
(25) Kulicke, W. M.; Kniewske, R. *Rheol. Acta* **1984**, *23*, 75.
(26) Janeschitz-Kriegl, H. *Polymer Melt Rheology and Flow Birefringence*; Springer-Verlag: New York, 1983.
(27) Menezes, E. V.; Graessley, W. W. *J. Polym. Sci., Polym. Phys. Ed.* **1982**, *20*, 1817.
(28) Attané, P.; Pierrard, J. M.; Turrel, G. *J. Non-Newtonian Fluid Mech.* **1985**, *18*, 295.
(29) Mead, D. W. In *Proceedings of the 12th International Congress on Rheology*, Aug 18−23, 1996; Aït-Kadi, A., Dealy, J. M., James, D. F., Williams, M. C., Eds.; Canadian Rheology Group: Quebec City, Canada, 1996.
(30) Pearson, D. S.; Kiss, A. D.; Fetters, L. J.; Doi, M. *J. Rheol.* **1989**, *33*, 517.
(31) McLeish, T. C. B.; Larson, R. G. *J. Rheol.* **1998**, *42*, 81.
(32) Marrucci, G.; de Cindio, B. *Rheol. Acta* **1980**, *19*, 68.
(33) Wagner, M. H. *Rheol. Acta* **1990**, *29*, 594.
(34) Wagner, M. H.; Schaeffer, J. *J. Rheol.* **1992**, *36*, 1.
(35) Watanabe, H.; Sakamoto, T.; Kotaka, T. *Macromolecules* **1985**, *18*, 1436.
(36) Montfort, J. P.; Marin, G.; Monge, P. *Macromolecules* **1984**, *17*,1551.
(37) Watanabe, H.; Urakawa, O.; Kotaka, T. *Macromolecules* **1994**, *27*, 3525.
(38) Viovy, J. L.; Monnerie, L.; Tassin, J. F. *J. Polym. Sci., Polym. Phys. Ed.* **1983**, *21*, 2427.
(39) Marrucci, G.; Ianniruberto, G. In *Dynamics of Complex Liquids*; Adams, M. J., Mashelkar, R. A., Pearson, J. R. A., Rennie, A. R., Eds.; Imperial College Press−The Royal Society: London, 1997.
(40) Einaga, Y.; Osaki, K.; Kurata, M.; Kimura, S.; Tamura, M. *Polym. J.* **1971**, *22*, 550.
(41) Osaki, K.; Nishizawa, K.; Kurata, M. *Macromolecules* **1982**, *15*, 1068.
(42) Osaki, K. *Rheol. Acta* **1993**, *32*, 429.
(43) Fukuda, M.; Osaki, K.; Kurata, M. *J. Polym. Sci., Polym. Phys. Ed.* **1975**, *13*, 1563.
(44) Vrentas, C. M.; Graessley, W. W. *J. Rheol.* **1982**, *26*, 359.
(45) Larson, R. G.; Khan, S. A.; Raju, V. R. *J. Rheol.* **1988**, *32*, 145.
(46) Morrison, F. A.; Larson, R. G. *J. Polym. Sci., Polym. Phys. Ed.* **1992**, *30*, 943.
(47) Archer, L. A.; Chen, Y.-L.; Larson, R. G. *J. Rheol.* **1995**, *39*, 519.
(48) Marrucci, G.; Grizzuti, N. *J. Rheol.* **1983**, *27*, 433.
(49) de Gennes, P.-G. *J. Phys. (Paris)* **1975**, *36*, 1199.
(50) Doi, M.; Kuzuu, N. Y. *J. Polym. Sci., Polym. Lett. Ed.* **1980**, *18*, 775.
(51) Pearson, D. S.; Helfand, E. *Macromolecules* **1984**, *17*, 888.
(52) Milner, S. T.; McLeish, T. C. B. *Macromolecules* **1997**, *30*, 2159.
(53) Fetters, L. J.; Lohse, D. J.; Richter, D.; Witten, T. A.; Zirkel, A. *Macromolecules* **1994**, *27*, 4639.
(54) Mead, D. W.; Larson, R. G. *Macromolecules* **1990**, *23*, 2524.

MA980127X